

**EXPERIENCE WITH THE SCALE CRITICALITY SAFETY
CROSS-SECTION LIBRARIES**

**S. M. Bowman
W. C. Jordan*
J. F. Mincey*
C. V. Parks
L. M. Petrie**

DRAFT

Date Published: April 2000

**Prepared by
OAK RIDGE NATIONAL LABORATORY
Oak Ridge, Tennessee 37831-6370
managed by
UT-BATTELLE, LLC
for the
U.S. DEPARTMENT OF ENERGY
under contract DE-AC05-00OR22725**

***Formerly with ORNL**

CONTENTS

	Page
LIST OF FIGURES	vii
LIST OF TABLES	ix
1. INTRODUCTION	1
2. GENERAL DISCUSSION	3
2.1 CROSS-SECTION GENERATION	3
2.2 RESONANCE PROCESSING	4
2.2.1 BONAMI	5
2.2.2 NITAWL	5
2.3 GENERAL DESCRIPTION OF THE VALIDATION EXPERIMENTS	6
2.3.1 High-Enriched Homogeneous ²³⁵ U Experiments	7
2.3.2 Low-Enriched Homogeneous ²³⁵ U Experiments	19
2.3.3 LWR Lattice Experiments	25
2.3.4 ²³⁹ Pu Experiments	28
2.3.5 ²³³ U Experiments	30
2.3.6 Mixed Oxide (MOX) Experiments	31
2.4 INTERPRETATION AND PRESENTATION OF CALCULATED RESULTS	33
3. THE SCALE 16-GROUP HANSEN-ROACH LIBRARY	35
3.1 ORIGINS OF THE LIBRARY	35
3.2 PERFORMANCE WITH HIGH-ENRICHED HOMOGENEOUS ²³⁵ U SYSTEMS	36
3.2.1 High-Enriched Fast Systems	36
3.2.2 High-Enriched Thermal Systems	36
3.2.3 High-Enriched Intermediate Spectrum Systems	36
3.3 PERFORMANCE WITH LOW-ENRICHED HOMOGENEOUS ²³⁵ U SYSTEMS	38
3.4 PERFORMANCE WITH LWR LATTICES	39
3.5 PERFORMANCE WITH ²³⁹ Pu SYSTEMS	40
3.6 PERFORMANCE WITH ²³³ U SYSTEMS	41
3.7 PERFORMANCE WITH MIXED OXIDE LATTICES	42
4. THE 218-GROUP ENDF/B-IV LIBRARY	43
4.1 ORIGINS OF THE LIBRARY	43
4.2 CHARACTERISTICS OF THE ENDF/B-IV LIBRARIES	43
4.3 PERFORMANCE WITH HIGH-ENRICHED HOMOGENEOUS ²³⁵ U SYSTEMS	44
4.3.1 High-Enriched Fast Systems	44
4.3.2 High-Enriched Thermal Systems	44
4.3.3 Intermediate Spectrum Systems	45
4.4 PERFORMANCE WITH LOW-ENRICHED HOMOGENEOUS ²³⁵ U SYSTEMS	46
4.5 PERFORMANCE WITH LWR LATTICES	47
4.6 PERFORMANCE WITH ²³⁹ Pu SYSTEMS	48

For a NUREG, page iii is the abstract (see Table 4.1 of NUREG-0650 Rev. 2).
Table of contents starts on page v.

4.7	PERFORMANCE WITH ^{233}U SYSTEMS	49
4.8	PERFORMANCE WITH MIXED OXIDE LATTICES	50
5.	THE 27-GROUP ENDF/B-IV LIBRARIES	51
5.1	ORIGINS OF THE 27-GROUP ENDF/B-IV LIBRARY	51
5.2	ORIGINS OF THE 27-GROUP BURNUP (DEPLETION) LIBRARY	51
5.3	CHARACTERISTICS OF THE ENDF/B-IV LIBRARIES	51
5.4	THERMAL-SCATTERING DATA LIMITATION	52
5.5	PERFORMANCE WITH HIGH-ENRICHED HOMOGENEOUS ^{235}U SYSTEMS	53
5.5.1	High-Enriched Fast Systems	53
5.5.2	High-Enriched Thermal Systems	53
5.5.3	Intermediate Spectrum Systems	53
5.6	PERFORMANCE WITH LOW-ENRICHED HOMOGENEOUS ^{235}U SYSTEMS	55
5.7	PERFORMANCE WITH LWR LATTICES	56
5.8	PERFORMANCE WITH ^{239}Pu SYSTEMS	57
5.9	PERFORMANCE WITH ^{233}U SYSTEMS	58
5.10	PERFORMANCE WITH MIXED OXIDE LATTICES	59
6.	THE 238-GROUP ENDF/B-V LIBRARY	61
6.1	ORIGINS OF THE LIBRARY	61
6.2	ENDF/B-VI DATA IN THE LIBRARY	61
6.3	PERFORMANCE WITH HIGH-ENRICHED HOMOGENEOUS ^{235}U SYSTEMS	63
6.3.1	High-Enriched Fast Systems	63
6.3.2	High-Enriched Thermal Systems	63
6.3.3	Intermediate Spectrum Systems	63
6.4	PERFORMANCE WITH LOW-ENRICHED HOMOGENEOUS ^{235}U SYSTEMS	65
6.5	PERFORMANCE WITH LWR LATTICES	66
6.6	PERFORMANCE WITH ^{239}Pu SYSTEMS	67
6.7	PERFORMANCE WITH ^{233}U SYSTEMS	68
6.8	PERFORMANCE WITH MIXED OXIDE LATTICES	70
7.	THE 44-GROUP ENDF/B-V LIBRARY	71
7.1	ORIGINS OF THE LIBRARY	71
7.2	ENDF/B-VI DATA IN THE LIBRARY	71
7.3	PERFORMANCE WITH HIGH-ENRICHED HOMOGENEOUS ^{235}U SYSTEMS	72
7.3.1	High-Enriched Fast Systems	72
7.3.2	High-Enriched Thermal Systems	72
7.3.3	Intermediate Spectrum Systems	72
7.4	PERFORMANCE WITH LOW-ENRICHED HOMOGENEOUS ^{235}U SYSTEMS	74
7.5	PERFORMANCE WITH LWR LATTICES	75
7.6	PERFORMANCE WITH ^{239}Pu SYSTEMS	76
7.7	PERFORMANCE WITH ^{233}U SYSTEMS	77
7.8	PERFORMANCE WITH MIXED OXIDE LATTICES	78
8.	SUMMARY AND CONCLUSIONS	79
8.1	SCALE 16-GROUP HANSEN-ROACH LIBRARY	80
8.2	SCALE 218-GROUP LIBRARY	80

*Make this page
Blank*



8.3	SCALE 27-GROUP LIBRARY	81
8.4	SCALE 238-GROUP LIBRARY	82
8.5	SCALE 44-GROUP LIBRARY	82
9.	REFERENCES	85
	APPENDIX A: SCALE CROSS-SECTION LIBRARY ENERGY-GROUP BOUNDARIES	87
	APPENDIX B: CALCULATIONAL BENCHMARKS	97
	B.1 DESCRIPTION OF THE BENCHMARKS	99
	B.1.1 PALMER BENCHMARKS	99
	B.1.2 Fe BENCHMARK	99
	B.1.3 UO ₂ F ₂ K-INFINITE CALCULATIONS	99
	B.1.4 PCTR EXPERIMENTS	100
	B.2 BENCHMARK RESULTS	100
	B.2.1 Performance of the SCALE 16-Group Hansen-Roach Library	100
	B.2.2 Performance of the SCALE 218-Group ENDF/B-IV Library	101
	B.2.3 Performance of the SCALE 27-Group ENDF/B-IV Library	101
	B.2.4 Performance of the SCALE 238-Group ENDF/B-IV Library	102
	B.2.5 Performance of the SCALE 44-Group ENDF/B-IV Library	102
	APPENDIX C: DETAILS OF THE HANSEN-ROACH LIBRARY	111
	APPENDIX D: DETAILS OF THE ENDF/B-IV LIBRARIES	117
	APPENDIX E: DETAILS OF THE ENDF/B-V LIBRARY	127
	APPENDIX F: CALCULATIONAL RESULTS	149

Start "Contents" on this page

Do not skip page between Content and Figures.

LIST OF FIGURES

Figure	Page
3.1	SCALE 16-group Hansen-Roach library high-enriched ²³⁵ U system results 37
3.2	SCALE 16-group Hansen-Roach library low-enriched homogeneous system results 38
3.3	SCALE 16-group Hansen-Roach library low-enriched LWR lattice results 39
3.4	SCALE 16-group Hansen-Roach library plutonium system results 40
3.5	SCALE 16-group Hansen-Roach library ²³³ U system results 41
3.6	SCALE 16-group Hansen-Roach library mixed oxide lattice results 42
4.1	SCALE 218-group ENDF/B-IV library high-enriched ²³⁵ U systems results 45
4.2	SCALE 218-group ENDF/B-IV library low-enriched homogeneous ²³⁵ U system results 46
4.3	SCALE 218-group ENDF/B-IV library low-enriched LWR lattice results 47
4.4	SCALE 218-group ENDF/B-IV library plutonium system results 48
4.5	SCALE 218-group ENDF/B-IV library ²³³ U system results 49
4.6	SCALE 218-group ENDF/B-IV library mixed oxide lattice results 50
5.1	SCALE 27-group ENDF/B-IV library high-enriched ²³⁵ U system results 54
5.2	SCALE 27-group ENDF/B-IV library low-enriched homogeneous ²³⁵ U system results 55
5.3	SCALE 27-group ENDF/B-IV library low-enriched LWR lattice results 56
5.4	SCALE 27-group ENDF/B-IV library plutonium system results 57
5.5	SCALE 27-group ENDF/B-IV library ²³³ U system results 58
5.6	SCALE 27-group ENDF/B-IV library mixed oxide lattice results 59
6.1	Weighting function for 238-group ENDF/B-V library 62
6.2	SCALE 238-group ENDF/B-V library high-enriched ²³⁵ U system results 64
6.3	SCALE 238-group ENDF/B-V library low-enriched homogeneous ²³⁵ U system results 65
6.4	SCALE 238-group ENDF/B-V library low-enriched LWR lattice results 66
6.5	SCALE 238-group ENDF/B-V library plutonium system results 67
6.6	SCALE 238-group ENDF/B-V library ²³³ U system results 68
6.7	SCALE 238-group ENDF/B-V library mixed oxide lattice results 69
7.1	SCALE 44-group ENDF/B-V library ²³⁵ U system results 73
7.2	SCALE 44-group ENDF/B-V library low-enriched homogeneous ²³⁵ U system results 74
7.3	SCALE 44-group ENDF/B-V library low-enriched LWR lattice results 75
7.4	SCALE 44-group ENDF/B-V library plutonium system results 76
7.5	SCALE 44-group ENDF/B-V library ²³³ U system results 77
7.6	SCALE 44-group ENDF/B-V library mixed oxide lattice results 78
B.1.	Palmer ²³⁵ U/metal mixture benchmark results 105
B.2.	Fully enriched UO ₂ F ₂ /H ₂ O <i>k-infinite</i> benchmark results 106
B.3	PCTR 1.006 wt% <i>k-infinite</i> experiments results 107
B.4	PCTR 1.071 wt% <i>k-infinite</i> experiment results 108
B.5	PCTR 1.157 wt% <i>k-infinite</i> experiment results 109

!!!!

Do not abbreviate between figures and tables

1. INTRODUCTION

SCALE¹ neutron cross-section libraries have seen widespread use over the years since the first release of SCALE in 1980. There have been numerous validation studies performed to satisfy ANSI/ANS-8.1-1998² and ANSI/ANS-8.17-1984³ but this information is scattered and not succinctly compiled into an easy-to-use format.

This report is intended to begin where the SCALE user manual leaves off in identifying performance of the SCALE libraries on various fissile systems. Some of the performance areas can be demonstrated by examining the performance of the libraries when calculating critical experiments. In areas where directly applicable critical experiments do not exist, other performance must be examined based on the general knowledge of the strengths and weaknesses of the cross sections. In this case, the experience in the use of the cross sections and comparisons to the results of other libraries on the same systems must be relied on for establishing acceptability of application of a particular SCALE library to a particular fissile system.

This report will aid in establishing when a SCALE cross-section library should perform acceptably and what areas of application should be more carefully scrutinized. To determine the acceptability of a library for a particular application, the calculational bias of the library should be established by directly applicable critical experiments. Preferably, the bias for a particular application should be small; however, if the bias and any trends in the bias are well defined, then the library should perform acceptably provided the bias and trends have been properly taken into account.

Table 1.1 shows the five neutron cross-section libraries currently available in SCALE. The SCALE Hansen-Roach library is a version of the Los Alamos 16-group Hansen-Roach library⁴ which has been modified at Oak Ridge National Laboratory (ORNL) and implemented into SCALE. The remaining four libraries were generated at ORNL for use as quasi system-independent criticality safety libraries. The group-wise energy boundaries for these libraries are presented in Appendix A.

Are you advocating code-to-code benchmarking?

Can be used

Table 1.1 SCALE cross-section libraries⁵

Actually 6 cross sections

Library	SCALE designator
SCALE 16-group Hansen-Roach	HANSEN-ROACH
218-group ENDF/B-IV ⁶	218GROUPNDF4
27-group ENDF/B-IV	27GROUPNDF4
27-group ENDF/B-IV Burnup Library	27BURNUPLIB
238-group ENDF/B-V ⁷	238GROUPNDF5
44-group ENDF/B-V ⁸	44GROUPNDF5

that

Some of the generic strengths and weaknesses of the SCALE libraries will be discussed in Sect. 2. Included in this section are some common characteristics of the libraries, and a discussion of the SCALE codes which perform resonance processing. Also included in Sect. 2 is a brief description of the calculational models and methodology used to demonstrate performance of the libraries.

2. GENERAL DISCUSSION

Some of the strengths and weaknesses of the SCALE libraries may be discussed in general terms. As an example, the strengths and weaknesses (assumptions and approximations) used in the codes which generate/process the SCALE cross sections become generic strengths and weaknesses of the SCALE cross-section libraries. BONAMI⁹ and NITAWL,¹⁰ the two codes used for resonance processing in SCALE, are discussed below. The manner in which a cross-section set is generated, including the processing code and assumed generating flux, also affects the performance of a library. An overview of common characteristics of the SCALE libraries is presented here.

In general, all of the SCALE libraries perform acceptably for unmoderated fast systems and hydrogen moderated thermal systems. These systems represent the largest class of application of the libraries and have the largest collection of critical experiments against which to validate. The SCALE libraries should be expected to perform less reliably for systems which have intermediate spectra and/or which have intermediate mass moderators that dominate the system transport, because of the lack of experimental data in these areas. As a final note here, it should be noted that many of the weaknesses of the SCALE libraries stem from weaknesses in the accuracy of the base data used to generate the libraries. Any library can perform only as well as the data upon which it is based. In the U.S., the current source for base cross-section data is the Evaluated Nuclear Data Files (ENDF) maintained at Brookhaven National Laboratory.

2.1 CROSS-SECTION GENERATION

Several factors affect the performance of multigroup cross-section libraries, regardless of the reliability of the base data. These factors include the number of energy groups, the location of the energy-group boundaries, the flux used to generate the cross-section library, and the methods used to self-shield resonance nuclides.

Two fine-group libraries have been generated and used extensively with SCALE. These are the CSRL 218-group ENDF/B-IV library and the LAW 238-group ENDF/B-V library. Both libraries were generated into an AMPX¹¹ master library format that contains all the needed information to further process the cross sections for problem-specific temperature and resonance effects (i.e., a problem-specific or working library). Thus, the AMPX master libraries are intended to be quasi-system independent criticality safety libraries. The problem-specific resolved resonance processing for both libraries (with the exception of a few nuclides) is via the Nordheim Integral Treatment within the NITAWL code. Single level Breit-Wigner resolved resonance (data is) carried on the AMPX master library for resonance nuclides.

The unresolved resonance region is processed at a fixed potential scattering cross section (σ_p) = 50,000 barns for the 218-group library. Using such a large value for σ_p results in insufficient self-shielding of the cross sections in the unresolved resonance region. For typical fast and thermal systems, this is not a problem. The unresolved resonance region in the 238-group library is handled by Bondarenko data, which is processed by BONAMI on a problem-specific basis.

The group structure for the fine-group libraries was developed for use on fast systems and thermal systems. Groups were intentionally included to subdivide resolved resonances of important nuclides (for example ²³⁸U) to minimize the effects of limitations of the Nordheim treatment within NITAWL on resonance processing. The additional energy group structure allows the resonance structure to be described in multigroup data similar to point data. Additional groups were added in going from the 218- to the 238-group library to specifically address the 0.3 eV thermal resonance in ²³⁹Pu that cannot be properly modeled in

*The data
is
plural
or singular?*

Additional to what?

NITAWL due to its low energy and lack of resonance data and the thermal Maxwellian peak. The additional 238- energy group structure also enables more accurate handling of thermal upscatter.

Repeat → The two fine-group libraries were generated with a different flux function, ~~and the differences can affect performance for certain classes of systems.~~ Resonance nuclides were generated with a fission Maxwellian (10 MeV to 70 keV) - 1/E (70 keV to 0.125 eV) - thermal Maxwellian (0.125 to 10⁻⁵ eV) flux function in both libraries. Nonresonance nuclides were generated with a fission Maxwellian - 1/(Eσ₀) - thermal Maxwellian flux function in the 218-group library and with a fission Maxwellian - 1/E - thermal Maxwellian flux function in the 238-group library. This difference in generating function can cause the two libraries to calculate differently for certain classes of systems.

Causing → The use of a weighting function 1/(Eσ₀) is analogous to processing cross-section structure with resonance self shielding based on the narrow resonance approximation. The use of a 1/E weighting function is analogous to processing the cross section at infinite dilution, thus providing no self shielding effect, ~~and~~ ^{but} the loss of resonance data. In the former case, the cross-section structure is highly shielded and in the latter it is totally unshielded. The significance of this lies in the fact that there are many nuclides in ENDF which have significant resonance structure but which, according to ENDF, are considered to be non-resonance nuclides. These nuclides are usually intermediate mass nuclides (e.g., Al, Si, S, Cl, K) and, if they play a significant role in the absorption and/or transport in a calculation, the two fine-group libraries can perform quite differently. The impact of the weighting on cross-section performance will be discussed more fully in the respective sections for the 218- and 238-group libraries.

The manner in which the ENDF/B-IV 27-group library and the ENDF/B-V 44-group library were collapsed from the parent fine-group libraries is also characteristically different. The 27-group library was collapsed using the generating flux of the 218-group library described above. This characteristic causes all nonresonance nuclides to have any cross-section structure fully self shielded; both capture and scatter cross sections are minimized. This characteristic is desirable for systems where a nuclide other than hydrogen dominates the transport (intermediate spectrum), but has little impact on fast or well-thermalized systems.

The 44-group library was collapsed using a typical light-water reactor lattice spectrum at room temperature conditions. This spectrum is very similar to an infinite dilute 1/E spectrum except that structure due to oxygen and ²³⁸U cross-section structure appears in the collapsing flux. The group structure of the library is the same as the 27-group library except that additional groups have been added below 0.4 eV to address the ²³⁹Pu resonance region (0.2 - 0.4 eV) and the thermal Maxwellian (0.003 - 0.1 eV). The library performs well on fast or well-thermalized systems and for lattices of fuel pins. The use of an infinite dilute collapsing flux causes all nonresonance nuclides to have cross-section structure shielded at minimum values. Both capture and scatter cross sections are maximized which adversely impacts some classes of homogeneous systems and systems where nuclides other than hydrogen dominate the transport.

2.2 RESONANCE PROCESSING

are able to ← BONAMI only used on unresolved resonances in SCALE.

Resonance processing in the SCALE sequences is performed by BONAMI and NITAWL. Each of these codes processes both resolved and unresolved resonance data using different methods discussed in the following sections. A common trait between both modules is that neither BONAMI nor NITAWL treat resonance overlap or resonance interference. Resonance overlap may occur because of several characteristics of a system. Typically, resonance overlap occurs when two nuclides in a mixture have resonances at the same or nearly the same energies as discussed in Sect. M7.A of the SCALE manual.¹ When resonance overlap is ignored, the flux used to shield the cross section is incorrect and thus the group cross section can be in error. Another form of resonance overlap can occur when the same resonance nuclide appears in

different regions (mixtures) of a geometry specification, because SCALE currently only processes one region at a time. Again, because an incorrect flux is used to shield the cross sections, the group cross sections can be in error. An example of this is in a dissolver where a fuel lump is surrounded by fissile solution containing the same resonance absorbers.

Resonance interference is similar to resonance overlap. When two resonances are close together, the higher energy resonance affects the flux shape in the lower energy resonance, because the flux does not reach the asymptotic flux form before the next resonance. Resonance interference can occur between resonances of different nuclides or two closely spaced resonances of the same nuclide. The limitations and approximations used in BONAMI and NITAWL will be discussed below.

NITAWL performs temperature broadening during resonance processing. If temperature data are included in the library, BONAMI performs temperature broadening at the user specified problem temperature during resonance processing. Starting with SCALE 4.3, NITAWL also performs a temperature interpolation of thermal scattering data on the master library.

Is data singular or plural?

2.2.1 BONAMI

The BONAMI module self shields cross sections with Bondarenko data using the shielding factor methodology. Nuclides with Bondarenko data carry an infinite dilute cross section on the master library and tables of shielding factors that are dilution dependent. BONAMI performs an iteration for each nuclide and each energy group that has shielding factors. Convergence is achieved when the sum of the individual shielded cross sections agrees with the shielded total cross section. In this manner, the problem-dependent self-shielded cross sections for each nuclide and each group are determined and interacting effects are taken into account. When CSAS calls BONAMI, heterogenous geometry effects are accounted in the escape cross section that is passed to BONAMI. It is determined based on the system geometry specified in the cross-section processing portion of the SCALE input. The geometry type, materials, characteristic dimensions, and Dancoff factor are all used to determine the escape cross section. By using the escape cross section to account for geometry effects, all nuclides can be processed by BONAMI as infinite homogeneous media in the CSAS sequences.

The escape cross section

for

The performance of libraries shielded by the Bondarenko method depends on the adequacy of the approximations used to generate the Bondarenko data. The typical approach is to use the narrow resonance approximation to generate these data, which is adequate for a broad range of applications. When a resonance is not narrow relative to the slowing down in the system, the narrow resonance approximation breaks down and the resonance corrections for the cross sections can be in error. This breakdown has been observed for libraries that use the Bondarenko method to shield the low energy resolved resonances for ^{238}U for systems with low hydrogen moderation and for many nuclides when the principle moderator is an intermediate mass nuclide. The solution to this type of breakdown is to either carry sufficient cross section energy groups to march across the resonance and/or to use more appropriate flux generating methods to compute the Bondarenko factors. This problem does not occur in the SCALE libraries because Bondarenko data are only used in the unresolved resonance range.

2.2.2 NITAWL

The NITAWL-II module shields cross sections with resonance data utilizing the Nordheim intergral transport method. In the SCALE implementation, the infinite dilute group cross sections are adjusted by a

correction value determined by NITAWL. The correction is calculated by first determining the infinite dilute contribution of each resonance to the group cross section and then by calculating what the contribution would be if the resonance was shielded for the specific problem. The geometry type, materials, characteristic dimensions, and Dancoff factor are all passed to NITAWL for determining the details of the approximations used to self shield the cross sections. NITAWL uses two moderators when reconstructing the shielded flux. The slowing down mass and scatter cross section for the principal material (first moderator) mixed with the fuel are used explicitly. The remaining materials (second moderator) are treated using an averaged slowing down mass and scatter cross section.

A fundamental assumption of the Nordheim method is that resonances are widely spaced, both within a particular nuclide and between nuclides. If this assumption is not correct, the flux used to construct the resonance contribution to the group cross section is incorrect. Breakdowns have been observed when NITAWL was used to self shield cross sections of fissile nuclides with overlapping resonances in dissolver type systems and in systems with intermediate mass moderators and intermediate mass resonance materials.

2.3 GENERAL DESCRIPTION OF THE VALIDATION EXPERIMENTS

In addition to discussing general experience and performance for each SCALE cross-section library, the performance of each library will be demonstrated for a set of benchmark models. These models are primarily composed of critical experiment models that have been used in the past to validate one or more of the SCALE libraries.

The performance of each library for these calculations provides a measure of the adequacy of the library. It is not surprising that, in general, the libraries perform rather predictably for these benchmarks; after all, most of the systems fall into the realm of typical applications. The calculations show the general range of application of the libraries. It cannot be emphasized too strongly that application of cross sections outside the range of validation must be done with great care, independent of the code and cross sections utilized. This is due to potential unidentified deficiencies in both the base cross-section data and in the manner the cross sections are manipulated for use by the various codes. *clarity*

The descriptions and results for several calculational benchmarks are presented in Appendix B. These calculational benchmarks are models that are hypothetical and do not model actual critical experiments, but were set up to study characteristics of the library over a range of parameters and allow for easy comparison of two or more cross-section libraries. Because they do not model an actual experiment, the calculational benchmarks do not demonstrate the adequacy of a particular code or cross-section set, but show over the range of possible application where different cross-section libraries agree or disagree. Agreement between the libraries for the various parametric studies does not, in itself, demonstrate the adequacy of the library for the application. Disagreement between libraries, however, does indicate where one or another of the libraries may be deficient. An obvious extension of this statement is that when different cross-section libraries give different results for the same system, similar differences should show up in the equivalent validations for the libraries; otherwise, neither library has been validated for the application.

2.3.1 High-Enriched Homogeneous ²³⁵U Experiments *and ?*

More than 130 critical experiments from Table 5 of ORNL/TM-238 (ref. 12) and the *International Handbook of Evaluated Criticality Safety Benchmark Experiments*¹³ (IHECSBE) were selected to evaluate the performance of the cross-section libraries for high-enriched homogeneous uranium systems. In addition, eight experiments using high-enriched uranium disks ~~of~~ polyethylene disks¹⁴ commonly referred to as the Jemima plates were selected. A list of the experiments is provided in Table 2.1. The experiments can be subdivided into three groups: (1) uranium metal systems with fast or intermediate energy spectra; (2) Jemima high-enriched experiments with intermediate spectra; and (3) uranyl nitrate and uranyl fluoride solutions with thermal energy spectra. These experiments are similar to those that have been used for criticality safety validation of weapons facilities. Six of the experiments in Table 5 were also included in the evaluated experiments of ref. 13. The evaluated models were used when available.

Table 2.1 High-enriched homogeneous ²³⁵U experiments

Case	Experimental description
CAS01*	Y-12 validation case A-1. 93.8% U metal sphere, unreflected (GODIVA)
CAS04	Y-12 validation case A-2. 93.2% U-Mo alloy cylinder annulus, unreflected
CAS05	Y-12 validation case A-3. 93.2% UO ₂ F ₂ solution, 19.992 g U/l, in Al sphere, unreflected
CAS06*	Y-12 validation case A-4. 93.18% UO ₂ (NO ₃) ₂ solution, 20.12 g U/l, in Al sphere, unreflected
CAS07	Y-12 validation case A-5. 93.5% U metal hemispherical shell, H ₂ O reflected
CAS08	Y-12 validation case A-6. 93.2% U metal cylinder annulus, graphite reflected
CAS09	Y-12 validation case A-7. 94% U metal cuboid, natural U reflected
CAS10	Y-12 validation case A-8. 93.1% U metal hemispherical shell, oil reflected
CAS11	Y-12 validation case A-9. 93.1 % U metal hemispherical shell, steel center and oil reflected

Table 2.1 High-enriched homogeneous ^{235}U experiments

Case	Experimental description
CAS14	Y-12 validation case B-11. 93.2% $\text{UO}_2(\text{NO}_3)_2$ solution, 505 g U/l, in SS cylinders, 4×4 array, standing in a solution slab, Plexiglas reflected
CAS15	Y-12 validation case B-12. 93.2% U metal cylinders, $2 \times 2 \times 2$ array, graphite moderated and polyethylene reflected
CAS19	Y-12 validation case B-16. 93.1% $\text{UO}_2(\text{NO}_3)_2$ solution, 450.8 g U/l, in SS containers, square central column with 8 perpendicular cylindrical arms unreflected
CAS20*	Y-12 validation case B-17. 93.17% $\text{UO}_2(\text{NO}_3)_2$ solution, 355.9 g U/l, in Al cylinders, 4×4 array, Plexiglas reflected
CAS21*	Y-12 validation case B-18. 93.17% $\text{UO}_2(\text{NO}_3)_2$ solution, 364.1 g U/l, in Al cylinders, 4×4 array, concrete reflected
CAS30	Problem S333SP0. 93.2% UO_2F_2 solution, 81.8 g U/l, in Al slabs, three 7.62 cm slabs in 3×1 array, 0 cm separation, unreflected, cylindrical tank, floor and walls in experiment room included
CAS32	Problem S333SP1. 93.2% UO_2F_2 solution, 81.8 g U/l, in Al slabs, three 7.62 cm slabs in 3×1 array, 2.54 cm separation, unreflected, cylindrical tank, floor, and walls in experiment room included
CAS34	Problem S333SP3. 93.2% UO_2F_2 solution, 81.8 g U/l, in Al slabs, three 7.62 cm slabs in 3×1 array, 7.62 cm separation, unreflected, cylindrical tank, floor, and walls in experiment room included

To this a letter or number?

Table 2.1 High-enriched homogeneous ^{235}U experiments

Case	Experimental description
CAS 36	Problem S333SP4. 93.2% UO_2F_2 solution, 81.8 g U/l, in Al slabs, three 7.62 cm slabs in 3×1 array, 11.43 cm separation, unreflected, cylindrical tank, floor, and walls in experiment room included
CAS38	Problem S333SP5. 93.2% UO_2F_2 solution, 81.8 g U/l, in Al slabs, three 7.62 cm slabs in 3×1 array, 13.97 cm separation, unreflected, cylindrical tank, floor, and walls in experiment room included
CAS40	Problem S333SP6. 93.2% UO_2F_2 solution, 81.8 g U/l, in Al slabs, three 7.62 cm slabs in 3×1 array, 15.24 cm separation, unreflected, cylindrical tank, floor, and walls in experiment room included
CAS31	Problem S333SP6R. 93.2% UO_2F_2 solution, 81.8 g U/l, in Al slabs, three 7.62 cm slabs in 3×1 array, 0 cm separation, H_2O reflected
CAS33	Problem S333SP1R. 93.2% UO_2F_2 solution, 81.8 g U/l, in Al slabs, three 7.62 cm slabs in 3×1 array, 2.54 cm separation, H_2O reflected
CAS35	Problem S333SP3R. 93.2% UO_2F_2 solution, 81.8 g U/l, in Al slabs, three 7.62 cm slabs in 3×1 array, 7.62 cm separation, H_2O reflected
CAS37	Problem S333SP4R. 93.2% UO_2F_2 solution, 81.8 g U/l, in Al slabs, three 7.62 cm slabs in 3×1 array, 11.43 cm separation, H_2O reflected

Is this a letter or number?

Table 2.1 High-enriched homogeneous ^{235}U experiments

Case	Experimental description
 CAS39	Problem S333SP5R. 93.2% UO_2F_2 solution, 81.8 g U/l, in A1 slabs, three 7.62 cm slabs in 3×1 array, 13.97 cm separation, H_2O reflected
CAS42	Problem S36SP2. 93.2% UO_2F_2 solution, 81.8 g U/l in A1 slabs, 7.62 cm and 14.834 cm slabs in 2×1 array, 5.08 cm separation, unreflected
CAS41	Problem S36SP15. 93.2% UO_2F_2 solution, 81.8 g U/l in A1 slabs, 7.62 cm and 14.834 cm slabs in 2×1 array, 38.1 cm separation, unreflected
CAS43	Problem S36SP30. 93.2% UO_2F_2 solution, 81.8 g U/l in A1 slabs, 7.62 cm and 14.834 cm slabs in 2×1 array, 76.2 cm separation, unreflected
CAS44	Problem S36SP48. 93.2% UO_2F_2 solution, 81.8 g U/l in A1 slabs, 7.62 cm and 14.834 cm slabs in 2×1 array, 121.92 cm separation, unreflected
CAS45	Problem S363SPO. 93.2% UO_2F_2 solution, 81.8 g U/l, in A1 slabs, 7.62 cm, 14.834 cm, and 7.62 cm slabs in 3×1 array, 0 cm separation, unreflected
CAS46	Problem S363SP10. 93.2% UO_2F_2 solution, 81.8 g U/l, in A1 slabs, 7.62 cm, 14.834 cm, and 7.62 cm slabs in 3×1 array, 25.4 cm separation, unreflected

Table 2.1 High-enriched homogeneous ^{235}U experiments

Case	Experimental description
CAS54	Problem S66SP2. 93.2% UO_2F_2 solution, 81.8 g U/l, in Al slabs. One slab is 14.834 cm, and the other is made up from two 7.62 cm slabs snugly fit together, 2×1 array, 5.08 cm separation, unreflected
CAS58	Problem S66SP6. 93.2% UO_2F_2 solution, 81.8 g U/l, in Al slabs. One slab is 14.834 cm, and the other is made up from two 7.62 cm slabs snugly fit together, 2×1 array, 15.24 cm separation, unreflected
CAS53	Problem S66SP15. 93.2% UO_2F_2 solution, 81.8 g U/l, in Al slabs. One slab is 14.834 cm, and the other is made up from two 7.62 cm slabs snugly fit together, 2×1 array, 38.1 cm separation, unreflected
CAS55	Problem S66SP20. 93.2% UO_2F_2 solution, 81.8 g U/l, in Al slabs. One slab is 14.834 cm, and the other is made up from two 7.62 cm slabs snugly fit together, 2×1 array, 50.8 cm separation, unreflected
CAS56	Problem S66SP30. 93.2% UO_2F_2 solution, 81.8 g U/l, in Al slabs. One slab is 14.834 cm, and the other is made up from two 7.62 cm slabs snugly fit together, 2×1 array, 76.2 cm separation, unreflected
CAS57	Problem S66SP48. 93.2% UO_2F_2 solution, 81.8 g U/l, in Al slabs. One slab is 14.834 cm, and the other is made up from two 7.62 cm slabs snugly fit together, 2×1 array, 121.92 cm separation, unreflected

subscript

Table 2.1 High-enriched homogeneous ^{235}U experiments

Case	Experimental description
CAS59	Problem S66SP66. 93.2% UO_2F_2 solution, 81.8 g U/l, in Al slabs. One slab is 14.834 cm, and the other is made up from two 7.62 cm slabs snugly fit together, 2×1 array, 167.64 cm separation, unreflected
CAS91	Problem U6B271F. 92.6% $\text{UO}_2(\text{NO}_3)_2$ solution, 63.3 g U/l, in Plexiglas cylinders, $3 \times 3 \times 3$ array, unreflected, walls, floor, and tank in experiment room included
CAS60	Problem U2B271F. 92.6% $\text{UO}_2(\text{NO}_3)_2$ solution, 279 g U/l, in Plexiglas cylinders, $3 \times 3 \times 3$ array, unreflected, walls, floor, and tank in experiment room included <i>subscript</i> ✓
CAS61	Problem U2B81F. 92.6% $\text{UO}_2(\text{NO}_3)_2$ solution, 279 g U/l, in Plexiglas cylinders, $2 \times 2 \times 2$ array, unreflected, walls, floor, and tank in experiment room included
CAS62	Problem U4B1251F. 92.6% $\text{UO}_2(\text{NO}_3)_2$ solution, 415 g U/l, in Plexiglas cylinders, $5 \times 5 \times 5$ array, unreflected, walls, floor, and tank in experiment room included
CAS64	Problem U4B641F. 92.6% $\text{UO}_2(\text{NO}_3)_2$ solution, 415 g U/l, in Plexiglas cylinders, $4 \times 4 \times 4$ array, unreflected, walls, floor, and tank in experiment room included

Table 2.1 High-enriched homogeneous ^{235}U experiments

Case	Experimental description
CAS63	Problem U4B271F. 92.6% $\text{UO}_2(\text{NO}_3)_2$ solution, 415 g U/l, in Plexiglas cylinders, $3 \times 3 \times 3$ array, unreflected, walls, floor, and tank in experiment room included
CAS65	Problem U4B81F. 92.6% $\text{UO}_2(\text{NO}_3)_2$ solution, 415 g U/l, in Plexiglas cylinders, $2 \times 2 \times 2$ array, unreflected, walls, floor, and tank in experiment room included
CAS90	Problem U4U2B27. 92.6% $\text{UO}_2(\text{NO}_3)_2$ solution, 415 g U/l, in Plexiglas cylinders, $3 \times 3 \times 3$ array, unreflected, 279 g U/l in 5 central units, walls, floor, and tank in experiment room included
CAS66	Problem U4R27A1 F. 92.6% $\text{UO}_2(\text{NO}_3)_2$ solution, 415 g U/l, in Plexiglas cylinders, $3 \times 3 \times 3$ array, reflected, 15.24 cm paraffin on bottom, 1.27 cm Plexiglas on other faces
CAS67	Problem U4R27B1F. 92.6% $\text{UO}_2(\text{NO}_3)_2$ solution, 415 g U/l, in Plexiglas cylinders, $3 \times 3 \times 3$ array, reflected, 15.24 cm paraffin on bottom, 2.54 cm Plexiglas on other faces
CAS68	Problem U4R27C1F. 92.6% $\text{UO}_2(\text{NO}_3)_2$ solution, 415 g U/l, in Plexiglas cylinders, $3 \times 3 \times 3$ array, reflected, 15.24 cm paraffin on bottom, 1.27 cm Plexiglas on other faces
CAS69	Problem U4R27D1F. 92.6% $\text{UO}_2(\text{NO}_3)_2$ solution, 415 g U/l, in Plexiglas cylinders, $3 \times 3 \times 3$ array, reflected, 15.24 cm paraffin on 5 faces, 15.24 cm Plexiglas on 1 face

What is the difference?

Table 2.2. Low-enriched homogeneous ^{235}U experiments

Case	Experimental description
CAR07	4.46% enriched U_3O_8 , $\text{H}/\text{U} = 0.77$, driven by high concentration (14.844 kg 351.18 g/l) fuel cans, plastic reflected
CAR08	4.46% ^{also?} enriched U_3O_8 , $\text{H}/\text{U} = 0.77$, driven by low concentration (12.871 kg 86.42 g/l) 93.17% enriched $\text{UO}_2(\text{NO}_3)_2$, 119 + 2S fuel cans, plastic reflected
CAR09	4.46% enriched U_3O_8 , $\text{H}/\text{U} = 0.77$, driven by low concentration (13.001 kg 86.42 g/l) 93.17% enriched $\text{UO}_2(\text{NO}_3)_2$, 119 + 2S fuel cans, plastic reflected
CAR10	4.46% enriched U_3O_8 , $\text{H}/\text{U} = 0.77$, driven by low concentration (12.446 kg 86.42 g/l) 93.17% enriched $\text{UO}_2(\text{NO}_3)_2$, 119 + 2S fuel cans, concrete reflected
CAR11	Experiment A. 4.46% enriched U_3O_8 , $\text{H}/\text{U} = 1.25$, 38 fuel cans with 2.44 cm interstitial moderation, plastic reflected
CAR12	Experiment B. 4.46% enriched U_3O_8 , $\text{H}/\text{U} = 1.25$, 78 fuel cans with 0.929 cm interstitial moderation, plastic reflected
CAR13	Experiment C. 4.46% enriched U_3O_8 , $\text{H}/\text{U} = 1.25$, 80 fuel cans with 0.929 cm interstitial moderation, plastic reflected
CAR14	4.46% enriched U_3O_8 , $\text{H}/\text{U} = 1.25$, driven by high concentration (12.268 kg 351.64 gU/l), 93.17% enriched $\text{UO}_2(\text{NO}_3)_2$, 119 + 2S fuel cans, plastic reflected
CAR15	4.46% enriched U_3O_8 , $\text{H}/\text{U} = 1.25$, driven by high concentration (12.400 kg 351.65 gU/l), 93.17% enriched $\text{UO}_2(\text{NO}_3)_2$, 119 + 2S fuel cans, plastic reflected

U233-MET-FAST-006

Natural?
Benchmark Critical Experiment of a ²³³U Sphere Reflected By
Normal Uranium with Flattop

U233-SOL-THERM-002

Paraffin-Reflected 8-, 8.5-, 9-, 10-, and 12-Inch-Diameter Cylinders of
²³³U Uranyl Nitrate Solutions

Experiment #	Cylinder Diameter (in.)	Solution Height (cm)
4	8	16.5195
5	8	16.8195
8	8	18.9195
22	8	14.8195
24	8	14.5195
34	8	16.8195
35	8	19.4195
10	8.5	19.5253
11	8.5	21.6253
12	9	21.4331
36	9	23.0331
14	10	19.4482
15	10	
38	10	
17	12	
18	12	
19	12	

U233-SOL-THERM-004 Paraffin-Reflected 5, 6, and 7.5-Inch-Diameter Cylinders of ²³³U Uranyl Nitrate Solutions ✓

Experiment #	Cylinder Diameter (in.)	Solution Height (cm)
3	6	38.5880
6	6	46.8880
20	6	30.7880
25	6	27.9880
30	6	29.0880
27	7.5	16.4109
28	7.5	16.3109
33	7.5	18.7109

2.3.6 Mixed Oxide (MOX) Experiments

Critical experiment cases 60 through 77 from Table 4.1 of NUREG/CR-6102 (ref. 8) were used to evaluate the performance of the SCALE codes and cross sections for mixed oxide systems. These experiments include both LWR and fast reactor type mixed oxide fuel pin lattices. The experiments are listed in Table 2.7.

3. THE SCALE 16-GROUP HANSEN-ROACH LIBRARY

3.1 ORIGINS OF THE LIBRARY

The SCALE 16-group Hansen-Roach library is based on the original Los Alamos report by Hansen and Roach. It is the only library discussed in this report that was not generated at ORNL. The original Hansen-Roach library was modified for easy use in the SCALE system. Several important nuclides not available in the original library were added by collapsing the 27-group ENDF/B-IV library to the 16-group structure of the Hansen-Roach library. The 16-group Hansen-Roach energy group structure is shown in Appendix A and a list of available nuclides in the library, and the source of the data for each nuclide is provided in Appendix C.

The Hansen-Roach library was primarily developed for fast ^{235}U systems. There are 12 fast groups and 4 thermal groups (below 3 eV). However, thermal upscatter was not included in the original Hansen-Roach data. It has been included in the nuclides added for SCALE, although most of those are heavy nuclides where thermal upscatter is not important. The original cross sections are generally P_0 cross sections that are transport corrected to account for leakage. Two exceptions are hydrogen and deuterium, which are P_1 with P_2 transport corrections. All of the nuclides later added to the original library were generated to the P_3 scattering order. One other significant improvement to the original library was made by Knight's modifications where multipliers for the ^{235}U capture cross section were generated as a function of background cross section based on three sets of low-enriched critical experiments. This last modification was key to extending the use of Hansen-Roach library to thermal low-enriched uranium systems.

Resonance nuclides in the original Hansen-Roach library had cross sections tabulated at several σ_p values. Prior to the development of the CSAS sequences in SCALE, the selection of one of these pre-processed shielded cross-section sets at Oak Ridge¹⁷ was made by hand calculation of σ_p for the problem of interest and the user then selecting the closest shielded cross-section set. When the Hansen-Roach library was incorporated into SCALE, the calculation of σ_p was automated. The method used to calculate σ_p and to select the shielded cross-sections will impact the performance of the Hansen-Roach library. The SCALE methodology has been used for the calculations discussed here.

In SCALE, σ_p is calculated on a group-wise basis using the total cross section. Cross-section shielding is then done on a group-wise basis with standard SCALE cross section processing modules; in particular, the BONAMI module.

To make the original Hansen-Roach cross sections compatible with the SCALE system, an infinite dilution set was defined for each resonance nuclide and Bondarenko data were generated for the remaining values of σ_p . This required generation of a 16-group total cross section for each nuclide to allow BONAMI to perform automatic problem-dependent cross-section processing. The original Hansen-Roach library did not carry total cross sections, per se, but contained a total cross section that included a transport correction. In order to implement the Hansen-Roach cross sections in SCALE, an infinitely dilute 16-group total cross section was generated from the SCALE 27-group library and added to the Hansen-Roach library as MT-201. The Bondarenko iteration scheme in BONAMI automatically uses MT-201 when it is present in a cross-section library; this feature permitted the original SCALE control modules to use BONAMI with the Hansen-Roach library.

Another characteristic of the Hansen-Roach library is that two sets of hydrogen cross sections are available; the dE/E set and the $\chi(E)$ set. These cross sections use different weighting schemes in the fast region. Historically, the $\chi(E)$ hydrogen was intended for fast systems and the dE/E hydrogen was intended for thermal systems. In SCALE, dE/E hydrogen is used by default in the standard compositions which

Give a quick description of the "infinite dilute" set.

It would be helpful at some place in a foot note to describe "infinite dilute."

3.5 PERFORMANCE WITH ^{239}Pu SYSTEMS

Extra space

The performance of the SCALE 16-group Hansen-Roach library for ^{239}Pu systems is shown in Fig. 3.4. The performance of the library is generally poor. The library shows an overall 2% positive bias with a +1% to -3% variation. This bias is probably due to poor thermal cross sections and inadequate group structure and resonance data. There are strong localized trends in the thermal region and the intermediate spectrum region which would be difficult to take into account for systems that are not closely related to the validation experiments.

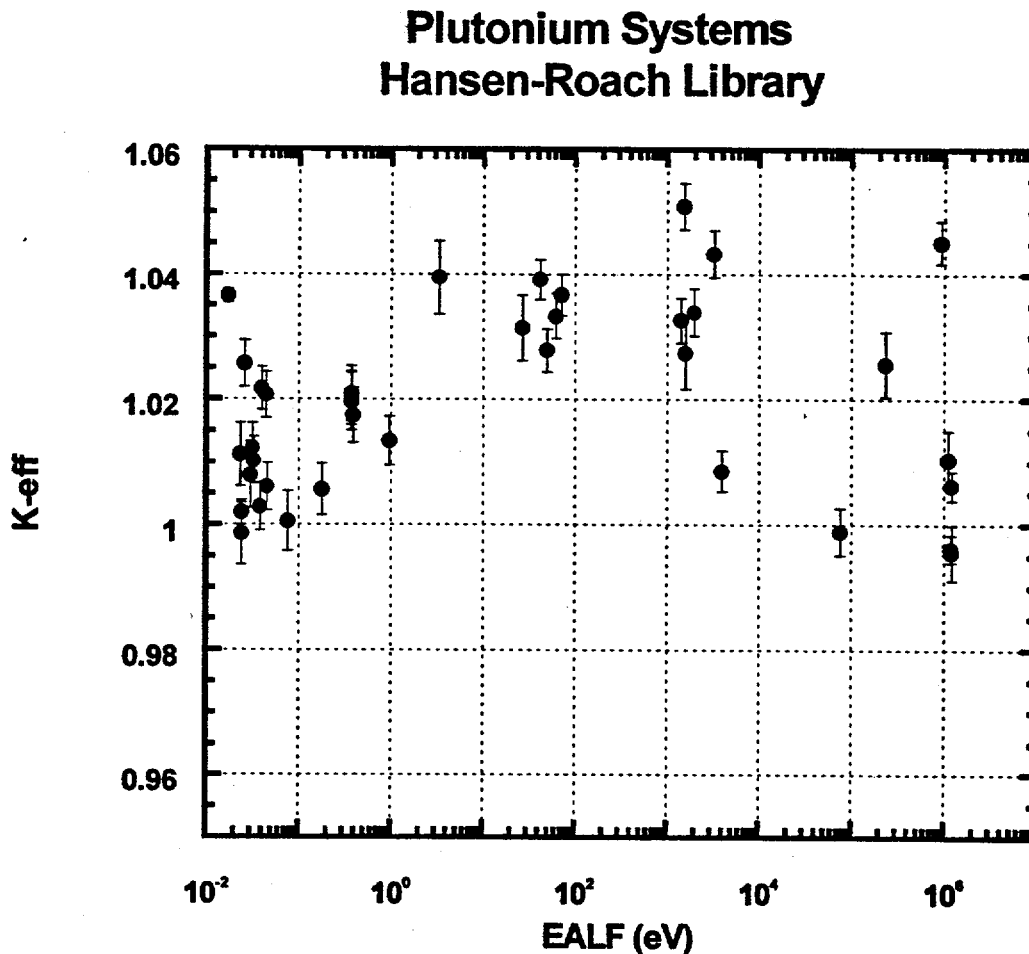


Fig. 3.4. SCALE 16-group Hansen-Roach library plutonium system results.

4. THE 218-GROUP ENDF/B-IV LIBRARY

4.1 ORIGINS OF THE LIBRARY

The 218-group ENDF/B-IV library was the most complete library available in SCALE prior to the release of the SCALE ENDF/B-V libraries in SCALE 4.3. The source of the data was ENDF/B-IV, and the processing of the cross sections by XLACS in the AMPX system is well documented.⁶ The weighting function used in the P_3 cross-section generation was a fission- $1/(E\sigma_f)$ -Maxwellian weighting [except for resonance nuclides, which were weighted $1/E$ instead of $1/(E\sigma_f)$]. The base weighting allowed the library to be successfully collapsed using the weighting spectrum to a broad group structure that could reproduce the behavior of the fine group library. One of the features of the library is that explicit resonance data carried with it can be used to generate problem-dependent, resolved resonance region multigroup cross sections using NITAWL-II. This capability allows great flexibility in the use of the library as a general-purpose criticality safety analysis library. Only the s-wave resonances are contained explicitly. Any p- and d-wave resonances were integrated into the background cross section. The library has 140 fast groups and 78 thermal groups (below 3.05 eV). The group structure was designed to fit the cross-section variation and reaction thresholds of the light and intermediate nuclides and to fit the major resonances of the intermediate and heavy nuclides. No unresolved resonance data are carried in the library. The unresolved resonance region was processed at a $\sigma_p = 50,000$ barns. early

The 218-group library has not been routinely validated because of its size and the related costs. However, the 27-group ENDF/B-IV library was derived directly from the 218-group library and has been validated against a large number of critical experiments (see Sect. 5). The 218-fine-group structure of the library generally will give either the same or more precise results than its companion 27-broad-group library.

An obvious advantage of a fine-group library over a broad-group library is that the library is less sensitive to the weighting spectrum used to generate the library. The cross sections more closely represent the base data, and the group structure allows a more detailed determination of the energy dependence of the flux. In past validations, it has been found useful to compare a fine-group calculation against a broad-group calculation when bias is observed. Appendix D contains a complete listing of the 218-group library nuclides as well as those nuclides that have resonance data or thermal scattering data.

4.2 CHARACTERISTICS OF THE ENDF/B-IV LIBRARIES

The ENDF/B-IV libraries have generally displayed a negative bias of approximately 1%, and in some cases as much as 2%, for low-enriched, water-moderated UO_2 rods. The bias appears to be greatest for epithermal systems (e.g., borated water and/or closely spaced rods) and less significant for more thermalized systems. The bias has been traced to the lack of data in the unresolved resonance region for ^{238}U in ENDF/B-IV. The unresolved resonance region in the SCALE ENDF/B-IV libraries was processed at $\sigma_p = 50,000$ barns, which is extremely high compared to σ_p values of 3500 barns for ^{235}U and 65 barns for ^{238}U in a typical LWR lattice. Improved data in ENDF/B-V eliminated this bias in the 44-group library. ✓

A positive bias has been routinely observed in the ENDF/B-IV libraries for thermal ^{239}Pu systems and mixed oxide (MOX) fuel rods. The MOX fuel rod bias increases with increasing thermalization. One problem identified in the 27-group library was inadequate group structure to account for flux changes across

4.8 PERFORMANCE WITH MIXED OXIDE LATTICES

The performance of the SCALE 218-group ENDF/B-IV library for mixed oxide lattices is shown in Fig. 4.6. All of the mixed oxide lattice systems considered here are water-moderated thermal systems. The performance of the library is fair, probably due to the ENDF/B-IV resonance data for ^{239}Pu . The most thermalized systems (about 0.1 eV) show a small positive bias, with results ranging from 0.995 to 1.01. As the spectrum becomes harder, the calculated k_{eff} values show an increasingly negative bias, similar to that seen for the LWR lattices.

*more like
0.990*

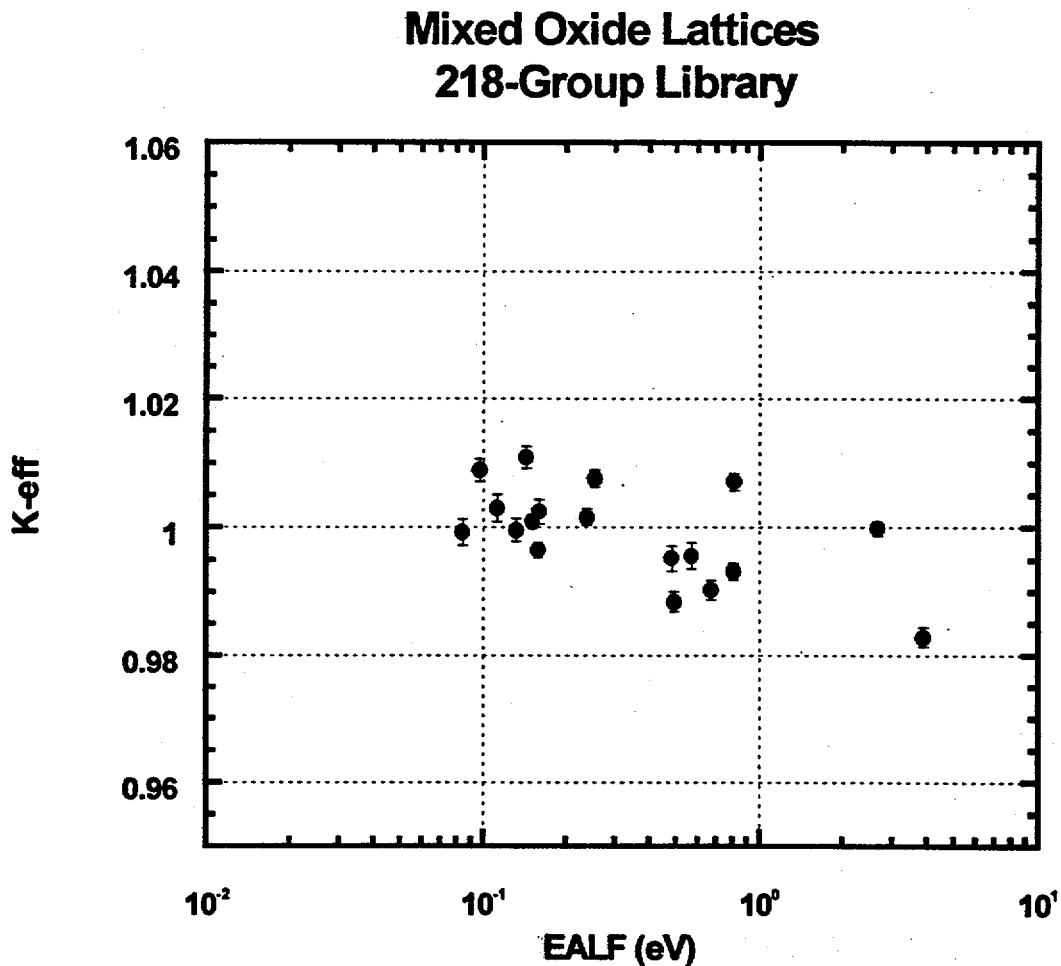


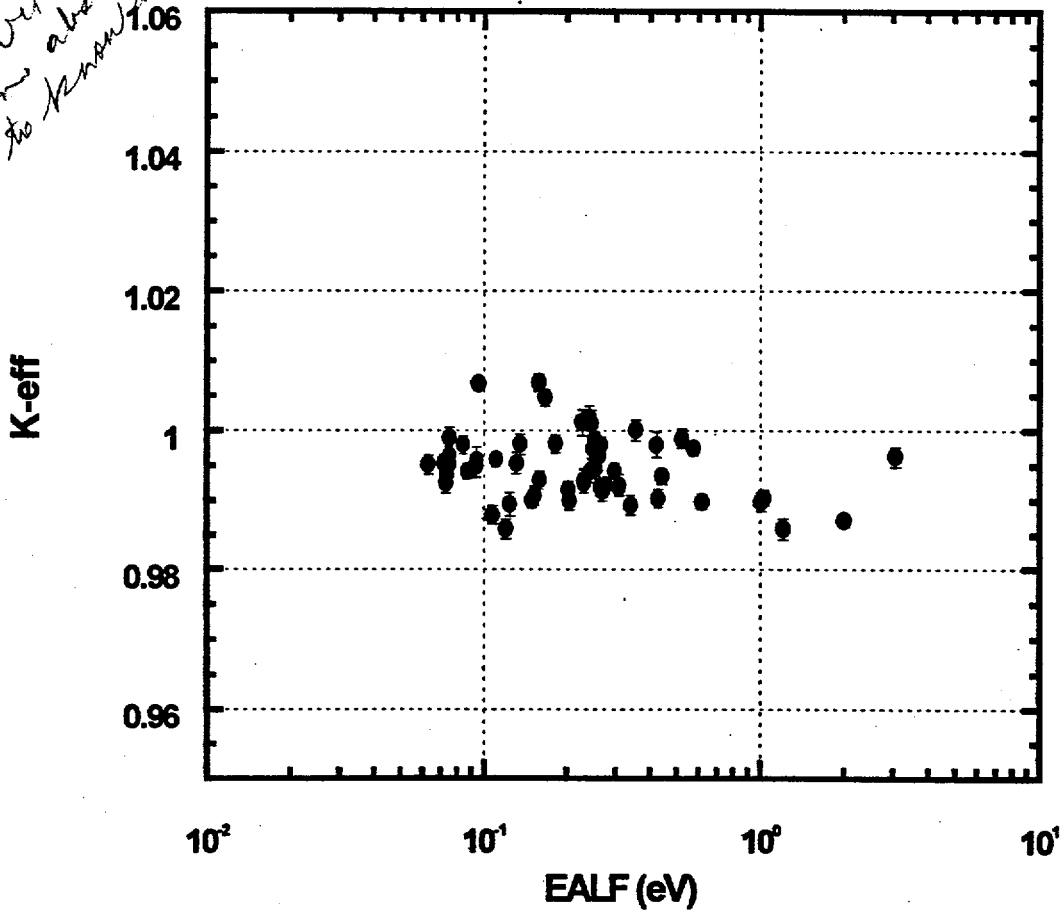
Fig. 4.6. SCALE 218-group ENDF/B-IV library mixed oxide lattice results.

5.7 PERFORMANCE WITH LWR LATTICES

The performance of the SCALE 27-group ENDF/B-IV library for heterogeneous low-enriched LWR lattice systems is shown in Fig. 5.3. The maximum enrichment in the LWR lattice experiments is 5.74 wt% ^{235}U . The experiments have an average k_{eff} of about 0.995 with a $\pm 1\%$ variation, about 0.5% more positive than the 218-group library results. The trend of lower calculated k_{eff} values for harder thermal spectra is consistent with previous LWR fuel lattice validation experience with the 27-group ENDF/B-IV library.

If any particular bias correlation has been observed for cases with boron absorber plates, we need to know about it. Solutions we apply here and for other libraries.

Low-Enriched UO₂ Lattices 27-Group Library



6. THE 238-GROUP ENDF/B-V LIBRARY

6.1 ORIGINS OF THE LIBRARY

The 238-group ENDF/B-V library is a general-purpose criticality analysis library, and the most complete library available in SCALE. This library is also known as the LAW (Library to Analyze Radioactive Waste) Library. The library contains data for all nuclides (more than 300) available in ENDF/B-V processed by the AMPX-77 system.¹⁴ It also contains data for ENDF/B-VI evaluations of ¹⁴N, ¹⁵N, ¹⁶O, ¹⁵⁴Eu, and ¹⁵⁵Eu, as discussed in Sect. 6.2. The library has 148 fast groups and 90 thermal groups (below 3 eV). The group structure is listed in Appendix A.

Most resonance nuclides in the 238-group and 44-group ENDF/B-V libraries have resonance data (to be processed by NITAWL-II) in the resolved resonance range and Bondarenko factors (to be processed by BONAMI) for the unresolved range. Both libraries contain resolved resonance data for s-wave, p-wave, and d-wave resonances ($\ell = 0$, $\ell = 1$, and $\ell = 2$, respectively) as shown in Table E.1. These data can have a significant effect on results for undermoderated, intermediate-energy problems. Resonance structures in several light-to-intermediate mass nonresonance ENDF nuclides (i.e., ⁷Li, ¹⁹F, ²⁷Al, ²⁸Si) are accounted for using Bondarenko shielding factors. These structures can also be important in intermediate energy problems. Nuclides with thermal scattering data are listed in Table E.2. The ²³⁵U ENDF/B-V data has slightly too much fission, while the ²³⁸U data has slightly too much capture. Although better than the ENDF/B-IV data, the thermal plutonium data still appears to have problems. have?

All nuclides in the 238-group LAW Library use the same weighting spectrum, consisting of

1. Maxwellian spectrum (peak at 300 K) from 10^{-5} to 0.125 eV,
2. a 1/E spectrum from 0.125 eV to 67.4 keV,
3. a fission spectrum (effective temperature at 1.273 MeV) from 67.4 keV to 10 MeV, and
4. a 1/E spectrum from 10 to 20 MeV.

A plot of this spectrum is shown in Fig. 6.1. The use of this spectrum makes it difficult to collapse a general purpose broad-group library that is valid over a wide range of problems.

All nuclides use a P_3 Legendre expansion to fit the elastic and discrete level inelastic scattering processes in the fast range, thereby making the library suitable for both reactor and shielding applications. A P_3 fit was used for thermal-scattering. All other scattering processes use P_0 fits.

Data testing has been performed for 33 benchmarks,⁸ including 28 Cross Section Evaluation Working Group (CSEWG) benchmarks. Results obtained for these benchmarks are very close to those obtained by other data testers using different ENDF/B-V-based cross-section libraries. There is considerable improvement in the trend of k_{eff} vs leakage obtained with the use of the ENDF/B-VI oxygen evaluation.

6.2 ENDF/B-VI DATA IN THE LIBRARY

Because of the significantly improved and conservative behavior of the ENDF/B-VI ¹⁶O evaluation under conditions where higher-order scattering terms are important (e.g, high leakage geometries), this cross section has been included in the 238-group and 44-group libraries as the default for ¹⁶O. The ENDF/B-V evaluation is available within the library as cross-section number 801601, and may be copied into an AMPX master library using AJAX for subsequent use in calculations. Similarly, ENDF/B-VI evaluations of ¹⁴N and ✓

Add a space

and ^{15}N are included in the library; however, ENDF/B-V versions remain the default for these isotopes. The ENDF/B-VI nitrogen data were processed using the same methods used for ^{16}O and, like oxygen, were tested to see if significant differences between ENDF/B-V and ENDF/B-VI could be identified. No significant differences have been identified; however, because they had already been processed into AMPX master library format and were readily available, ENDF/B-VI ^{14}N and ^{15}N cross sections are included in the library as cross sections 701401 and 701501, respectively. Finally, ENDF/B-VI evaluations of ^{154}Eu and ^{155}Eu are also included in the library as default cross sections 63154 and 63155, respectively. The more recent ENDF/B-VI evaluations include resonance parameters not included in previous evaluations and yield energy-dependent cross sections significantly different from those obtained using ENDF/B-V cross sections. Comparisons of depletion/decay calculations to experimental isotopic measurements have indicated that the ENDF/B-VI europium evaluations are more accurate than those available in ENDF/B-V. However, as with ^{16}O , ENDF/B-V cross sections are available within the library, as isotopes 631541 and 631551.

Add a space

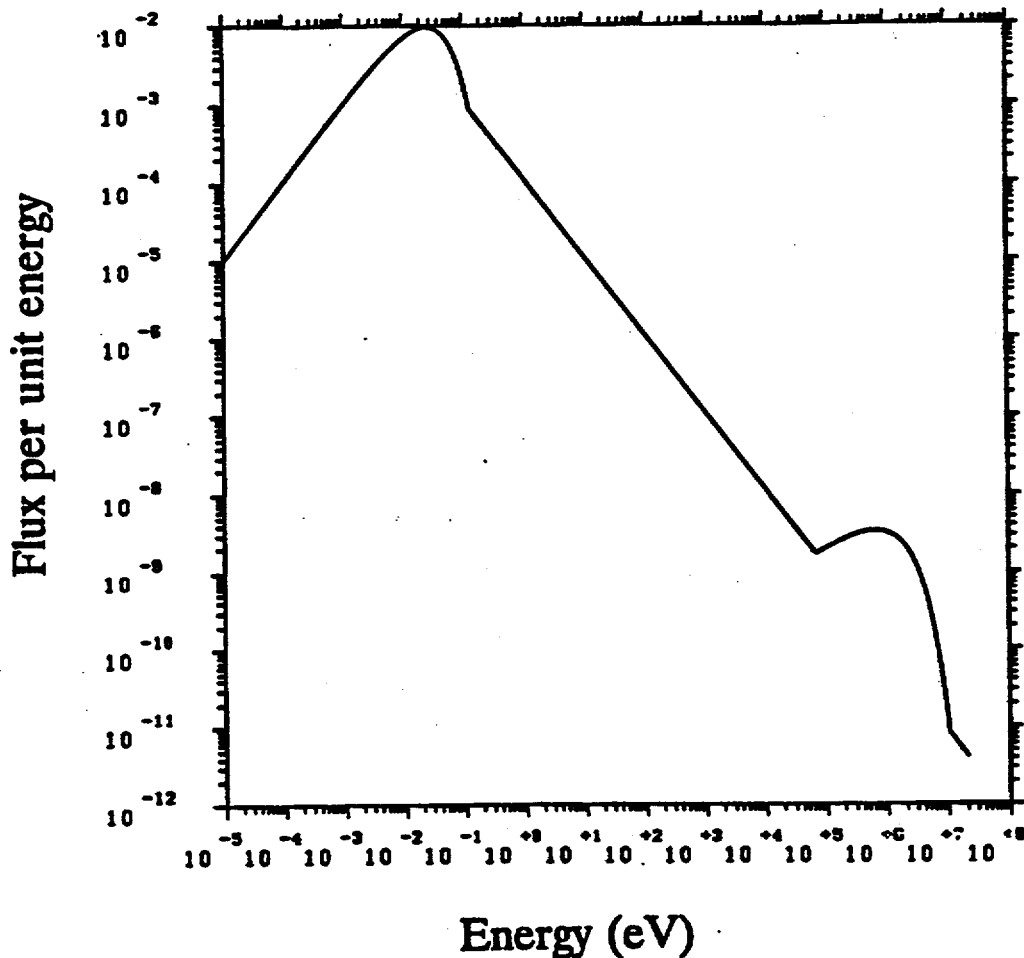


Fig. 6.1. Weighting function for 238-group ENDF/B-V library.

6.8 PERFORMANCE WITH MIXED OXIDE LATTICES

The performance of the SCALE 238-group ENDF/B-V library for mixed oxide lattices is shown in Fig. 6.7. All of the mixed oxide lattice systems considered here are water-moderated thermal systems. The performance of the library is very good. The average calculated k_{eff} value is approximately $0.995 \pm 1\%$. The results show a trend vs energy (i.e., moderation). The most thermal cases have a slightly positive bias, while those with a harder spectrum have a slightly negative bias.

Table 8.1
Page 1.0

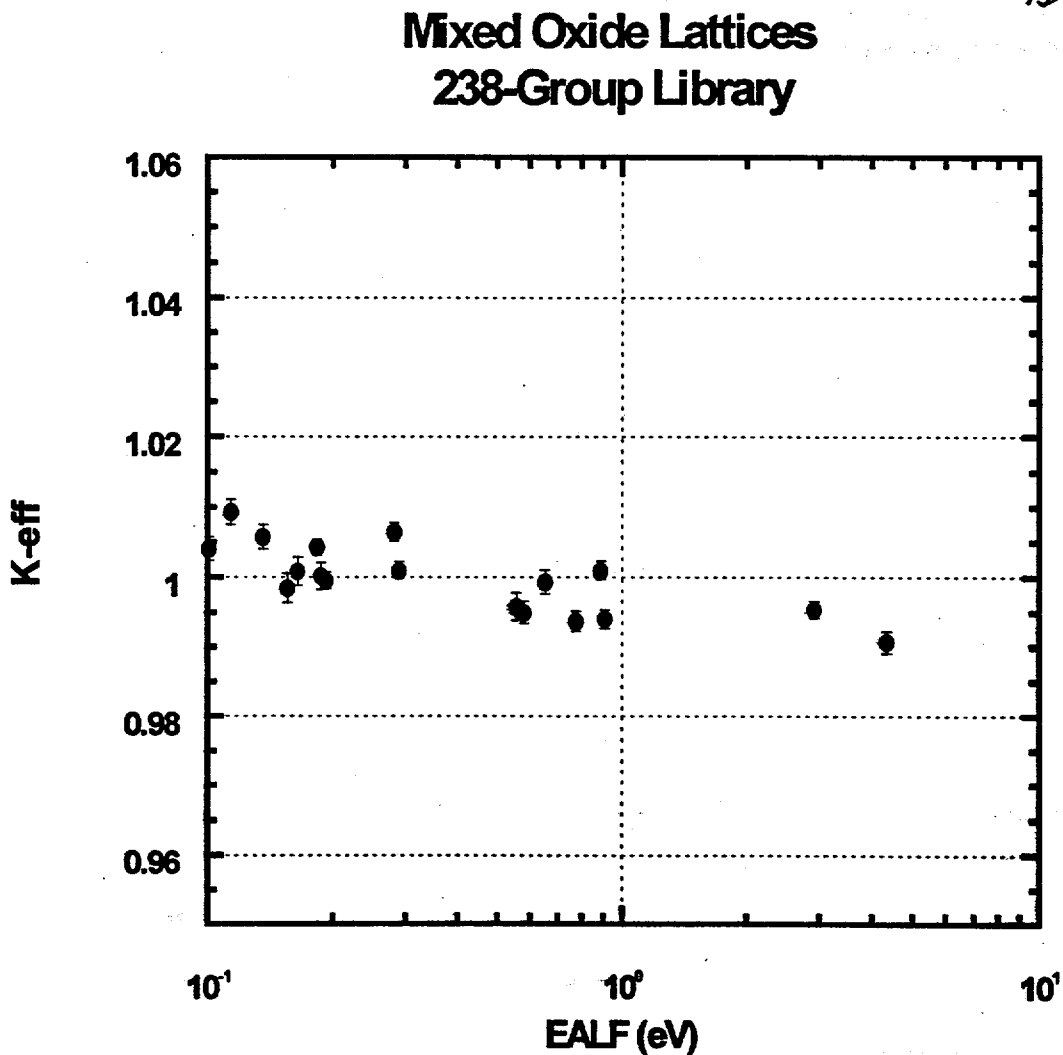


Fig. 6.7. SCALE 238-group ENDF/B-V library mixed oxide lattice results.

7. THE 44-GROUP ENDF/B-V LIBRARY

7.1 ORIGINS OF THE LIBRARY

The 44-group ENDF/B-V library has been developed for use in the analysis of fresh and spent fuel and radioactive waste systems. Collapsed from the fine-group 238-group ENDF/B-V cross-section library, this broad-group library contains all nuclides (more than 300) from the ENDF/B-V data files. Broad-group boundaries were chosen as a subset of the parent 238-group ENDF/B-V boundaries, emphasizing the key spectral aspects of a typical LWR fuel package. Specifically, the broad-group structure was designed to accommodate the following features: two windows in the oxygen cross-section spectrum; a window in the cross section of iron; the Maxwellian peak in the thermal range; and the 0.3-eV resonance in ^{239}Pu (which, due to its low energy, cannot be properly modeled via the SCALE Nordheim Integral Treatment module NITAWL-II). The resulting boundaries represent 22 fast and 22 thermal energy groups; the full group structure is compared to that of the 238-group library in Table A.1. The fine-group 238-group ENDF/B-V cross sections were collapsed into this broad-group structure using a fuel cell spectrum calculated based on a 17×17 Westinghouse pressurized-water reactor (PWR) assembly. Thus, the 44-group library performs well for LWR lattices, but not as well for other types of systems.

The 44-group ENDF/B-V library has been tested against its parent library using a set of 33 benchmark problems⁸ in order to demonstrate that the collapsed set was an acceptable representation of 238-group ENDF/B-V, except for intermediate energy systems. Validation of the library within the SCALE system was based on a comparison of calculated values of k_{eff} with that of 93 experiments: 92 critical and 1 subcritical experiments.⁸ The experiments primarily consisted of various configurations of light-water-reactor-type fuel representative of transportation and storage conditions. Additional experiments were included to allow comparison with results obtained in earlier validation of the 27-group ENDF/B-IV library.

Results show that the broad 44-group structure is an acceptable representation of its parent 238-group library for thermal LWR lattice systems as well as hard fast spectrum systems. The 44-group library is the recommended SCALE library for criticality safety analysis of arrays of light-water-reactor-type fuel assemblies, as would be encountered in fresh or spent fuel transportation or storage environments. Validation results for LWR-type UO_2 fuel show virtually no bias. A positive bias of 0.5 to 1% has been observed for very thermal mixed-oxide systems. The bias is caused by inadequate representation of plutonium cross sections, possibly in the ENDF/B-V data. These validation results are consistently better than those seen for the same cases using the 27-group ENDF/B-IV library. Because of the weighting spectrum used to collapse the 238-group library, it is difficult to collapse a general purpose broad-group library that is valid over a wide range of problems. For all other systems, the parent 238-group ENDF/B-V library is recommended.

7.2 ENDF/B-VI DATA IN THE LIBRARY

Because of the significantly improved and conservative behavior of the ENDF/B-VI ^{16}O evaluation under conditions where higher-order scattering terms are important (e.g. high leakage geometries), this cross section has been included in the 238-group and 44-group libraries as the default for ^{16}O . The ENDF/B-V evaluation is available within the library as cross-section number 801601, and may be copied into an AMPX working library using AJAX for subsequent use in calculations. Similarly, ENDF/B-VI evaluations of ^{14}N

and ^{15}N are included in the library; however, ENDF/B-V versions remain the default for these isotopes. The ENDF/B-VI nitrogen data were processed using the same methods used for ^{16}O , and, like oxygen, were tested to see if significant differences between ENDF/B-V and ENDF/B-VI could be identified. No significant differences have been identified; however, because they had already been processed into AMPX master library format and were readily available, ENDF/B-VI ^{14}N and ^{15}N cross sections are included in the library as cross sections 701401 and 701501, respectively. Finally, ENDF/B-VI evaluations of ^{154}Eu and ^{155}Eu are also included in the library as default cross sections 63154 and 63155, respectively. The more recent ENDF/B-VI evaluations include resonance parameters not included in previous evaluations and yield energy-dependent cross sections significantly different from those obtained using ENDF/B-V cross sections. Comparisons of depletion/decay calculations to experimental isotopic measurements have indicated that the ENDF/B-VI europium evaluations are more accurate than those available in ENDF/B-V. However, as with ^{16}O , ENDF/B-V cross sections are available within the library, as isotopes 631541 and 631551.

7.3 PERFORMANCE WITH HIGH-ENRICHED HOMOGENEOUS ^{235}U SYSTEMS

Figure 7.1 shows calculated k_{eff} values for highly enriched ^{235}U systems using the SCALE 44-group ENDF/B-V library. The overall trend shows an average k_{eff} of approximately 1.00 for thermal and fast systems, with a large variation in results for thermal systems.

7.3.1 High-Enriched Fast Systems

Fast systems in Fig. 7.1 are represented by the group of calculations at an EALF of 8×10^5 eV or greater. The fast systems have an average k_{eff} of about 0.995 with a variation of about $\pm 1\%$, very similar to the 238-group library results.

7.3.2 High-Enriched Thermal Systems

Thermal systems in Fig. 7.1 are represented by the calculations with an EALF below about 3 eV. The average k_{eff} in the thermal region is about 1.00 with a variation of roughly $\pm 2\%$. There is a wide spread of results in the thermal range ($k_{\text{eff}} < 0.98$ to $k_{\text{eff}} > 1.03$). Similar spreads can be seen in the results for the other libraries, too. As observed with the other libraries, the uranyl fluoride results tend to be less than the uranyl nitrate results. The possibility of large uncertainties in the specifications for the critical systems used to validate the thermal range cannot be ruled out as the source of the large variations in calculated k_{eff} values.

7.3.3 High-Enriched Intermediate Spectrum Systems

Intermediate spectrum systems in Fig. 7.1 are those with an EALF between 3 eV and 8×10^5 eV. There are few critical experiments in the intermediate range. These systems are characterized by an ill defined average k_{eff} of $1.00 \pm 1.5\%$. Some cases are roughly 1% higher while others are nearly the same as the 238-group results.

8. SUMMARY AND CONCLUSIONS

This report provides detailed information on the SCALE criticality safety cross-section libraries. Areas covered include the origins of the libraries, the data on which they are based, how they were generated, past experience and validations, and performance comparisons to measured critical experiments and numerical benchmarks. Performance results of each library for seven different application areas are summarized in Table 8.1.

The remainder of this section contains a brief verbal summary of each library.

Table 8.1 Summary of SCALE library performance for various applications

Problem Type	Cross-section library				
	Hansen-Roach	27-group * ENDF/B-IV	218-group * ENDF/B-IV	44-group ENDF/B-V	238-group ENDF/B-V
Fast HEU	very good 0.995 ± 1%	very good 1.00 ± 1%	very good 1.00 ± 1%	very good ^{0.72} 1.00 ± 1% _{0.995}	very good 0.995 ± 1%
Thermal HEU	very poor 2% high to 4% low	poor 3% high to 2% low	poor 1.00 ± 2%	poor 1.00 ± 3%	poor 1.00 ± 2%
LWR Lattices	fair ± 1.5%	good 0.995 ± 1% small bias vs energy	good 0.99 ± 1% small bias vs energy	very good 1.00 ± 1%	very good 0.995 ± 1%
Homogeneous LEU	poor ± 2% bias vs energy	fair 1.00 ± 1.5%	fair 0.995 ± 1.5%	fair 1.01 ± 1.5%	fair 1.005 ± 1.5%
²³⁹ Pu	very poor up to 5% high bias vs energy	poor up to 5% high bias vs energy	poor up to 5% high bias vs energy	fair 1.02 ± 2%	fair 1.02 ± 2% <i>P.67 says 1.015.</i>
MOX lattices	very poor 3% high to 1% low	fair 1.00 ± 1.5% bias vs energy	fair 1% high to 2% low bias vs energy	excellent 1.003 ± 0.6%	very good 1.00 ± 1% small bias vs energy
²³⁵ U	poor thermal - 0.99 ± 2% fast - 1.0 ± 1%	poor thermal - 1.02 ± 1.5% fast - 0.97 ± 1%	poor thermal - 1.015 ± 1.5% fast - 0.97 ± 1%	good Thermal 1.00 ± 1.5% Fast - 0.997 ± 0.5%	good Thermal - 0.995 ± 1.5% Fast - 0.999 ± 0.4%

* Use of hafnium and gadolinium data not recommended.

8.1 SCALE 16-GROUP HANSEN-ROACH LIBRARY

1. How the library was generated or collapsed:

The library was generated from available data of 1960 vintage. It was originally intended for fast calculations (6 fast groups), and later extended to 16 groups covering the full energy range. For the fast range, the cross section values seem to have been pretty much "eyeballed," while a flat lethargy flux was used for integrating the intermediate range. Most of the data is P_0 transport corrected data, but hydrogen and deuterium are P_1 data with a P_2 transport correction. The ^{235}U data in the resonance range ~~was~~ *were* adjusted to give good results for the PCTR experiments and the ORNL green block experiments. ✓

2. Known biases/weaknesses in original data for this library:

The age and sparseness of the base data are the major weakness. Temperature effects and thermal upscatter are not treated.

3. Application areas where the library performs well:

The library performs well for small high-enriched ^{235}U metal systems and fairly well for many uranium thermal systems. LEU ✓

4. Application areas where the library performs poorly:

Thermal HEU
Optimally moderated uranyl nitrate solutions underpredict by as much as 2.5 to 3% in k_{eff} . Plutonium systems may be high by 2 to 4%. Thermal ^{233}U systems can underpredict k_{eff} by 2 to 3%.

8.2 SCALE 218-GROUP LIBRARY

1. How the library was generated or collapsed:

This library was generated from ENDF/B-IV data using $\chi(E)-1/(E\sigma_0)$ -Maxwellian weighting. The base weighting allowed the library to be successfully collapsed using the weighting spectrum to a broad group structure that could reproduce the behavior of the fine group library. The unresolved resonance region was processed with an extremely high background cross section of 50,000 barns, resulting in infinite dilution cross sections in this region. Only the s-wave resonances were carried on the library, and any p-wave and d-wave resonances were integrated into the background cross section. The processing of the unresolved resonances with the extremely high background cross section and the integration of the higher angular momentum p- and d-wave resolved resonances into the background cross section resulted in too much absorption in the intermediate energy range.

2. Known biases/weaknesses in original data for this library:

The ^{238}U base data had too much capture in the epithermal range, leading to underprediction of k_{eff} for low enriched systems. The graphite thermal kernel was deficient, with unknown results.

harder flux in

is

3. Application areas where the library performs well:

This library performs well for most realistic criticality safety problems. Fast, small metal units, highly enriched thermal systems, and very thermal low enriched systems are generally well predicted.

4. Application areas where the library performs poorly:

Low enriched systems with a hard thermal spectrum underpredict by approximately 1% and sometimes more. Plutonium thermal systems overpredict k_{eff} by 1.5 to 3%. The 218-group library overpredicts thermal ^{233}U systems by about 2%, while it underpredicts fast ^{233}U systems by 2 to 4%. Intermediate energy systems, such as the Palmer problems, can be wrong by large amounts.

8.3 SCALE 27-GROUP LIBRARY

1. How the library was generated or collapsed:

The 27-group library was collapsed from the 218-group library using the weighting spectra with which the nuclides were originally generated. Because of the $1/(E\sigma)$ weighting in the resonance range, the broad group library calculates many systems nearly as well as the fine group library does. Trends and biases in the fine group library were preserved in the broad group library.

2. Known biases/weaknesses in original data for this library:

Same as the 218-group library.

3. Application areas where the library performs well:

Generally the same as the 218-group library. Some trends and biases may be slightly more pronounced in the broad group library, but most results are fairly equivalent.

4. Application areas where the library performs poorly:

Same as the 218-group library.

8.4 SCALE 238-GROUP LIBRARY

1. How the library was generated or collapsed:

The library was generated from ENDF/B-V data using a $\chi(E)$ -1/E-Maxwellian spectrum. The integrating function makes it more difficult to collapse a general purpose broad-group library that is valid over a large range of problems. It contains all nuclides (over 300) in ENDF/B-V plus data for ENDF/B-VI evaluations of ^{14}N , ^{15}N , ^{16}O , ^{154}Eu , and ^{155}Eu .

2. Known biases/weaknesses in original data for this library:

The ^{235}U fission data and the ^{238}U capture data are slightly too high. There may be a problem with the thermal plutonium cross sections.

3. Application areas where the library performs well:

Generally this library has done very well for high-enriched fast systems and low-enriched thermal homogeneous and lattice systems. Results for mixed oxide lattices and ^{233}U systems are good, too. This library is recommended as the best library in SCALE for general purpose criticality safety analyses.

Add a space

4. Application areas where the library performs poorly:

This library has problems with intermediate energy problems involving nuclides with cross section structure without resonance parameters. Although any intermediate energy problems are suspect because of the scarcity of critical experiments, this library performs better than any other library in SCALE.

8.5 SCALE 44-GROUP LIBRARY

1. How the library was generated or collapsed:

This library was collapsed from the 238-group library using a LWR flux spectrum. Consequently, the library does well predicting LWR lattices, but not as well for other types of systems.

2. Known biases/weaknesses in original data for this library:

Same as the 238-group library. Because of the 1/E weighting in the 238-group library, this library is not a good general purpose library.

APPENDIX A

SCALE CROSS-SECTION LIBRARY ENERGY-GROUP BOUNDARIES

Table A.1 SCALE cross-section library energy-group boundaries

ENDF/B-V 238-group	ENDF/B-IV 218-group	ENDF/B-V 44-group	ENDF/B-IV 27-group	Hansen-Roach 16-group	Upper energy (eV)
1	1	1	1		2.0000E+07
2					1.7333E+07
3					1.5683E+07
4					1.5000E+07
5					1.4550E+07
6					1.3840E+07
7				1	1.0000E+07
8		2			8.1873E+06
9	2	3	2		6.4340E+06
10	3	4			4.8000E+06
11	4				4.3040E+06
12	5	5	3	2	3.0000E+06
13	6	6			2.4790E+06
14	7	7			2.3540E+06
15	8	8	4		1.8500E+06
16	9				1.5000E+06
17	10	9	5	3	1.4000E+06
18	11				1.3560E+06
19	12				1.3170E+06
20	13				1.2500E+06
21	14				1.2000E+06
22	15				1.1000E+06
23	16				1.0100E+06
24	17				9.2000E+05
25	18	10	6	4	9.0000E+05
26	19				8.7500E+05
27	20				8.6110E+05
28	21				8.2000E+05
29	22				7.5000E+05
30	23				6.7900E+05
31	24				6.7000E+05
32	25				6.0000E+05

APPENDIX B

CALCULATIONAL BENCHMARKS

B.1 DESCRIPTION OF THE BENCHMARKS

B.1.1 Palmer Benchmarks

The Palmer benchmarks consist of three calculational benchmarks that were devised to study the performance of various cross-section sets for calculating *k-infinite* for ^{235}U /metal mixtures. The following systems are considered: $^{235}\text{U}/\text{Al}$ at an $\text{Al}/^{235}\text{U}$ atom ratio of 2470, $^{235}\text{U}/\text{Fe}$ at an $\text{Fe}/^{235}\text{U}$ atom ratio of 320, and $^{235}\text{U}/\text{Zr}$ at a $\text{Zr}/^{235}\text{U}$ atom ratio of 103. These systems were originally developed to have a *k-infinite* = 1.0 utilizing the ENDF/B-V cross sections in MCNP. Subsequent study of these cases indicated significant deficiencies in ENDF/B-V cross sections, the T2 evaluation of iron in MCNP, and in cross section processing in the SCALE codes. The best estimates of the "correct results" are *k-infinite* = 1.12 ± 0.04 , 1.09 ± 0.04 , and 1.11 ± 0.04 for the Al, Fe, and Zr systems, respectively. There are no experiments which validate the reliability of the cross sections for these applications. The large uncertainties indicate the uncertainties expected from the known deficiencies in the cross sections.

B.1.2 Fe Benchmark

The Fe benchmark is another calculational benchmark which identified deficiencies in the SCALE resonance processing for Fe. The benchmark is a simplification of the critical experiment HMF-035 into a simple unreflected $^{235}\text{U}/\text{Fe}$ sphere, 107. cm radius, at an $\text{Fe}/^{235}\text{U}$ atom ratio = 63.2 ($N_{\text{Fe}}=8.13913\text{-}2$, $N_{\text{U-235}}=1.28882\text{-}3$) The best estimate of the "correct k_{eff} " for this sphere is 1.00 ± 0.02 . The benchmark complements the Palmer benchmarks and shows how calculational performance for an infinite system is not necessarily indicative of performance for a finite system.

B.1.3 UO_2F_2 *K-Infinite* Calculations

The UO_2F_2 *k-infinite* calculations are a series of calculational benchmarks which span a moderation range from $\text{H}/\text{X}=0$ to 700. The benchmarks were developed to study fully enriched $\text{UO}_2\text{F}_2/\text{H}_2\text{O}$ systems. This series of benchmarks was used to identify significant deficiencies in the SCALE 123 group cross-section library and ultimately led to the removal of the library from SCALE. The "expected value" was determined using MCNP and ENDF/B-V cross sections for uranium, fluorine, and hydrogen, and ENDF/B-VI oxygen. An uncertainty of 0.5% in the expected k_{eff} values was assigned to the series of calculations.

Should this be
 k -infinity?

B.1.4 PCTR Experiments

The PCTR benchmarks are a series of *k-infinite* measurements for low enriched ^{235}U which were performed in the Physical Constant Test Reactor at Hanford. The experiments were designed to help predict the minimum enrichment which could be made critical in a homogeneous light water moderated system. These experiments provide a good test of the ^{235}U cross sections and have been used to identify deficiencies in the Hansen-Roach cross-section library for low enriched uranium systems.

B.2 BENCHMARK RESULTS

A comparison of the performance of the SCALE cross-section libraries for these calculational benchmarks is presented in this section. This gives a birds-eye view of how the various SCALE cross-section libraries compare with each other for ^{235}U systems across a range of interest. This series of benchmarks includes the Palmer problems, the Fe sphere, $\text{U}(100)\text{O}_2\text{F}_2$ *k-infinite* calculations, and the PCTR low-enriched uranium *k-infinite* experiments. All of these calculations with the exception of the PCTR experiments are numerical (i.e., calculational) benchmarks for library comparison. The results presented here may be used to supplement the information presented in Sects. 3-6 of this report. *all five*

Table B.1 shows the results for ~~four~~ of the SCALE libraries. The "expected" k_{eff} value and an estimate of the uncertainty of the expected value are given. Except for the PCTR experiments, the expected value is a best estimate of the correct k for the specified system. The uncertainty has been assigned based on previous evaluation of these systems and general uncertainties encountered in the ENDF cross sections. The PCTR values are experimentally determined *k-infinite* values and uncertainties. Included in the table are the EALF (energy of average lethargy of the neutron causing fission), the calculated results and the ratio of the calculated to expected value.

Figure B.1 presents a comparison of results for the Palmer benchmarks. Note that the shift in the EALF is due to the combined effects of differences in cross sections and in averages performed over different group structures. Figure B.2 shows the results of the UO_2F_2 *k-infinite* calculations as a function of EALF. The SCALE 16-group Hansen-Roach library, which has only four thermal groups, exhibits the largest shifts in EALF. Figures B.3 - B.5 display the results for the three different enrichments of the PCTR experiments. Because no EALF data corresponding to the expected k_{eff} values are available, the expected k_{eff} values are plotted vs the 44-group library EALF values as a convenience.

B.2.1 Performance of the SCALE 16-group Hansen-Roach Library

The results in Table B.1 and Fig. B.1 show that the SCALE 16-group Hansen-Roach library calculated *k-infinite* values for the Palmer Al/U and Fe/U benchmarks are about 10% low. The Palmer Zr/U benchmark calculates about 25% high. These results are due to a combination of factors, including lack of resonance data for Al, Fe, and Zr cross sections and a broad group structure. The library should ~~be~~ not be used for applications where intermediate mass nuclides are the principle scattering materials or in intermediate spectrum systems where absorption is dominated by intermediate mass absorbers.

The high-enriched U/Fe sphere calculates 20% high where the Palmer Fe/U system calculates 10% low. This discrepancy demonstrates that flux-weighted multigroup cross sections as generated in AMPX cannot correctly model transport through thick materials with cross-section energy windows, such as iron. Errors on the order of up to 30% in k can exist for similar systems. *elaborate*

Figure B.2 shows that there may be a large variation in performance depending on the moderation level of the system. Calculated *k-infinite* values are 2% high when oxygen and fluorine are the principal moderators. Calculated *k-infinite* values are approximately 1% low over the intermediate spectrum range and trend to nominally unbiased for more thermal systems. This behavior indicates that the SCALE 16-group cross-section set should be used with caution in the intermediate-spectrum, hydrogen moderated systems.

Figures B.3 - B.5 show that there is a fairly consistent 2% positive bias for the PCTR low enriched uranium experiments. This bias is probably due to the broad group structure and inadequate resonance processing for this system.

B.2.2 Performance of the SCALE 218-group ENDF/B-IV Library

Table B.1 and Figure B.1 show that the SCALE 218-group library calculates from 10 to 25% low for the Palmer benchmarks. Poor performance for the Al/U benchmark can be primarily attributed to poor ENDF/B-IV cross sections for Al. Poor performance for the Fe systems is probably due to a combination of effects which include inadequate group structure, cross section generation methods, and resonance processing methodology. The Zr/U benchmark calculates low due to poor ENDF/B-IV cross sections for Zr and due to inadequate resonance processing in the SCALE 218-group library.

Similar to the Hansen-Roach library, the U/Fe sphere calculates nearly 20% high while the Palmer Fe/U system calculates 25% low. Once again, this difference in results indicates the use of flux weighting to generate multigroup cross sections will not conserve the neutron transport for this type system unless the group structure is extremely fine across the resonance region of Fe. It is difficult to conserve both the reaction rate and the transport for systems similar to the U/Fe sphere. *Should there be a warning against using for iron systems?*

Figure B.2 shows that the SCALE 218-group library performs adequately across the range of the UO₂F₂ *k-infinite* benchmarks. The library shows a 0.5% positive bias across the intermediate spectrum, and a -0.5% bias for the most thermal systems.

Figures B.3-B.5 show that the SCALE 218-group library calculates these low enriched uranium systems approximately 1% low. This is primarily due to poor ENDF/B-IV²³⁸U cross sections and inadequate unresolved resonance region processing in the 218-group library.

B.2.3 Performance of the SCALE 27-group ENDF/B-IV Library

Table B.1 and Fig. B.1 show that the SCALE 27-group library calculates from 10 to 20% low for the Palmer benchmarks. Poor performance for the Al/U benchmark can be primarily attributed to poor ENDF/B-IV cross sections for Al. Poor performance for the Fe systems is probably due to a combination of effects which include inadequate group structure, cross section generation methods, and resonance processing methodology. The Zr/U benchmark calculates low due to poor ENDF/B-IV cross sections for Zr and due to inadequate resonance processing in the SCALE 27-group library.

Like the 218-group library, the U/Fe sphere calculates 20% high while the Palmer Fe/U system calculates 20% low. Once again, this difference in results indicates the use of flux weighting to generate multigroup cross sections will not conserve the neutron transport for this type system unless the group structure is extremely fine across the resonance region of Fe. *Add warning.*

Figure B.2 shows that the SCALE 27-group library performs adequately across the range of the UO₂F₂ *k*-infinite benchmarks. The results are virtually identical to the 218-group results. The library shows a 0.5% positive bias across the intermediate spectrum, and a -0.5% bias for the most thermal systems.

Figures B.3-B.5 show that the SCALE 27-group library calculates these low enriched uranium systems nominally 0.5 to 1% low. The results are slightly higher than the 218-group results. This is primarily due to poor ENDF/B-IV ²³⁸U cross sections and inadequate unresolved resonance region processing in the 27-group library.

B.2.4 Performance of the SCALE 238-group ENDF/B-V Library

Table B.1 and Figure B.1 show that the SCALE 238-group library calculates from 2 to 13% low for the Palmer benchmarks. While the Al/U results are very similar to the ENDF/B-IV libraries, the Fe/U and Zr/U are significantly better. The poor performance for the Al/U benchmark can be primarily attributed to lack of resonance data for Al in ENDF/B-V. Aluminum has significant resonance structure but is not considered a resonance nuclide in ENDF. The Fe/U benchmark is approximately 3% low, and the Zr/U benchmark is only 2% low.

The disparity in the 238-group library results for the U/Fe sphere (10% high) and the Palmer Fe/U system (3% low) is much smaller than the other libraries. As stated previously, it is difficult to conserve both the reaction rate and the transport for systems similar to the U/Fe sphere in a multigroup structure.

Figure B.2 shows that the SCALE 238-group library performs well across the range of the UO₂F₂ *k*-infinite benchmarks. The library shows almost no bias across the entire spectrum.

Figures B.3-B.5 show that the SCALE 238-group library calculates these low enriched uranium systems very well, within ±0.5%.

B.2.5 Performance of the SCALE 44-group ENDF/B-V Library

Table B.1 and Fig. B.1 show that the SCALE 44-group library calculates from 0 to 20% low for the Palmer benchmarks. The Al/U results are 10% lower than any other library. This difference is apparently due to the broad-group collapse of the 44-group library. The resonance structure for aluminum evidently occurs over several fine groups in the 238-group library that are collapsed to a single broad group in the 44-group library, causing the loss of that resonance structure. This problem does not occur in the 27-group library collapse because of the different weighting $[1/(E\sigma)]$ used in the 218-group library. As stated earlier in this report, the 1/E weighting of the resonance region in the 238-group library makes it difficult to collapse a general purpose broad-group library.

The Fe/U benchmark is approximately 4% low, and the Zr/U benchmark shows agreement with the expected value. The consistent Fe/U results between the 44- and 238-group libraries is due to the careful preservation of energy windows in the Fe cross sections in the 44-group structure.

The disparity in the 44-group library results for the U/Fe sphere (14% high) and the Palmer Fe/U system (4% low) is similar to the 238-group library. As stated previously, it is difficult to conserve both the reaction rate and the transport for systems similar to the U/Fe sphere in a multigroup structure.

Where are the EALF and and ratio of $\frac{\text{Calculated}}{\text{Expected}}$?

Table B.1 Computational benchmark results

Benchmarks	Expected k_{eff}	Uncertainty	Calc. k_{eff} (16 group)	Calc. k_{eff} (27 group)	Calc. k_{eff} (218 group)	Calc. k_{eff} (44 group)	Calc. k_{eff} (238 group)
Palmer Al/U	1.120E+00	4.000E-02	1.005E+00	1.021E+00	1.001E+00	8.808E-01	9.818E-01
Palmer Fe/U	1.090E+00	4.000E-02	1.003E+00	8.576E-01	8.193E-01	1.049E+00	1.055E+00
Palmer Zr/U	1.110E+00	4.000E-02	1.383E+00	1.027E+00	9.602E-01	1.117E+00	1.089E+00
High-enriched U/Fe sphere	1.000E+00	2.000E-02	1.203E+00	1.198E+00	1.169E+00	1.142E+00	1.105E+00
U(100)O ₂ F ₂ , h/x=0	2.087E+00	5.000E-03	2.133E+00	2.081E+00	2.076E+00	2.077E+00	2.085E+00
U(100)O ₂ F ₂ , h/x=5	1.795E+00	5.000E-03	1.797E+00	1.807E+00	1.802E+00	1.808E+00	1.804E+00
U(100)O ₂ F ₂ , h/x=10	1.796E+00	5.000E-03	1.785E+00	1.807E+00	1.800E+00	1.809E+00	1.803E+00
U(100)O ₂ F ₂ , h/x=20	1.836E+00	5.000E-03	1.819E+00	1.839E+00	1.834E+00	1.844E+00	1.840E+00
U(100)O ₂ F ₂ , h/x=50	1.892E+00	5.000E-03	1.876E+00	1.888E+00	1.885E+00	1.895E+00	1.894E+00
U(100)O ₂ F ₂ , h/x=100	1.898E+00	5.000E-03	1.884E+00	1.890E+00	1.889E+00	1.899E+00	1.898E+00
U(100)O ₂ F ₂ , h/x=200	1.843E+00	5.000E-03	1.835E+00	1.835E+00	1.834E+00	1.844E+00	1.844E+00
U(100)O ₂ F ₂ , h/x=300	1.775E+00	5.000E-03	1.771E+00	1.767E+00	1.767E+00	1.776E+00	1.776E+00
U(100)O ₂ F ₂ , h/x=500	1.643E+00	5.000E-03	1.645E+00	1.635E+00	1.635E+00	1.643E+00	1.643E+00
U(100)O ₂ F ₂ , h/x=700	1.526E+00	5.000E-03	1.532E+00	1.519E+00	1.519E+00	1.526E+00	1.526E+00
PCTR 1.006%, h/u=3.83	9.860E-01	5.000E-03	1.014E+00	9.807E-01	9.756E-01	9.894E-01	9.863E-01
PCTR 1.006%, h/u=6.23	9.860E-01	7.000E-03	9.978E-01	9.758E-01	9.727E-01	9.828E-01	9.815E-01
PCTR 1.006%, h/u=6.95	9.740E-01	5.000E-03	9.893E-01	9.683E-01	9.655E-01	9.749E-01	9.739E-01
PCTR 1.006%, h/u=7.52	9.600E-01	5.000E-03	9.812E-01	9.614E-01	9.588E-01	9.677E-01	9.669E-01
PCTR 1.071%, h/u=3.78	1.005E+00	6.000E-03	1.035E+00	1.001E+00	9.953E-01	1.010E+00	1.006E+00
PCTR 1.071%, h/u=5.84	1.005E+00	6.000E-03	1.025E+00	1.002E+00	9.987E-01	1.010E+00	1.008E+00
PCTR 1.071%, h/u=7.14	9.920E-01	7.000E-03	1.011E+00	9.902E-01	9.874E-01	9.970E-01	9.960E-01
PCTR 1.157%, h/u=3.73	1.031E+00	6.000E-03	1.059E+00	1.025E+00	1.019E+00	1.034E+00	1.030E+00
PCTR 1.157%, h/u=5.99	1.031E+00	5.000E-03	1.052E+00	1.029E+00	1.026E+00	1.037E+00	1.035E+00
PCTR 1.157%, h/u=6.90	1.030E+00	7.000E-03	1.043E+00	1.022E+00	1.019E+00	1.029E+00	1.028E+00
PCTR 1.157%, h/u=7.52	1.019E+00	5.000E-03	1.036E+00	1.016E+00	1.013E+00	1.022E+00	1.022E+00

Palmer Benchmarks

²³⁵U / Metal Mixtures

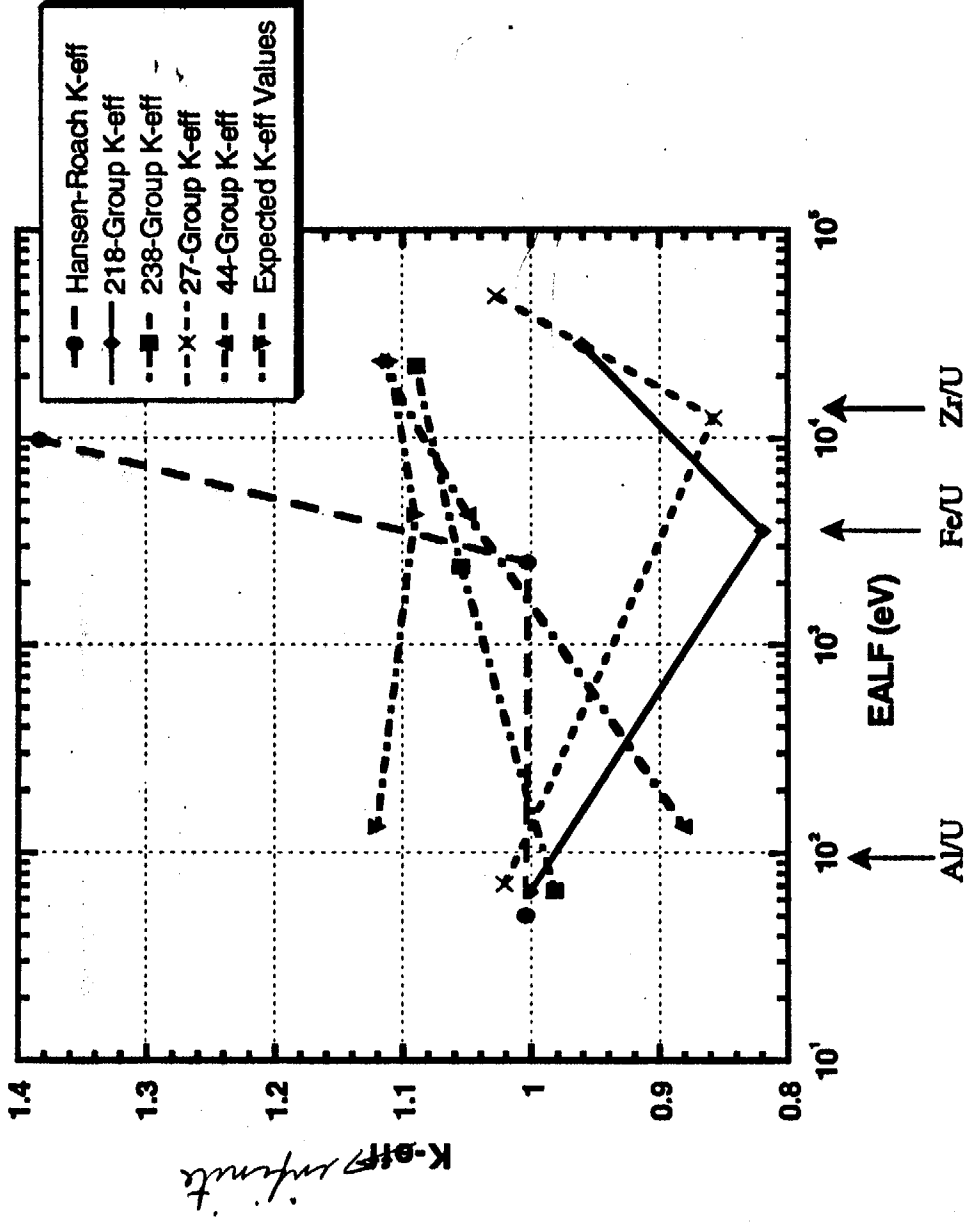


Fig. B.1. Palmer ²³⁵U/metal mixture benchmark results.

Fully Enriched UO₂F₂ / H₂O k-infinite Benchmarks

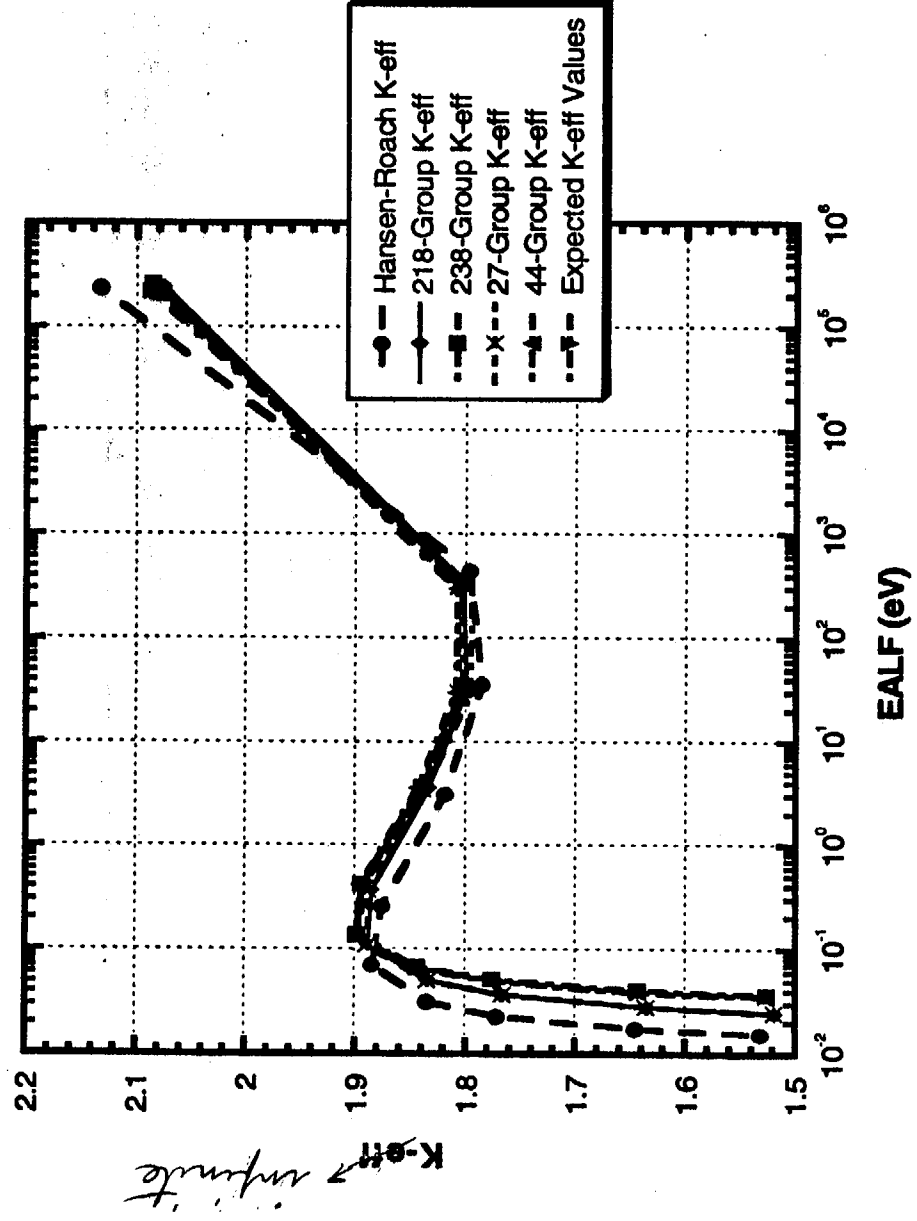


Fig. B.2. Fully enriched UO₂F₂/H₂O *k-infinite* benchmark results.

PCTR 1.006 wt % k-infinite Experiments

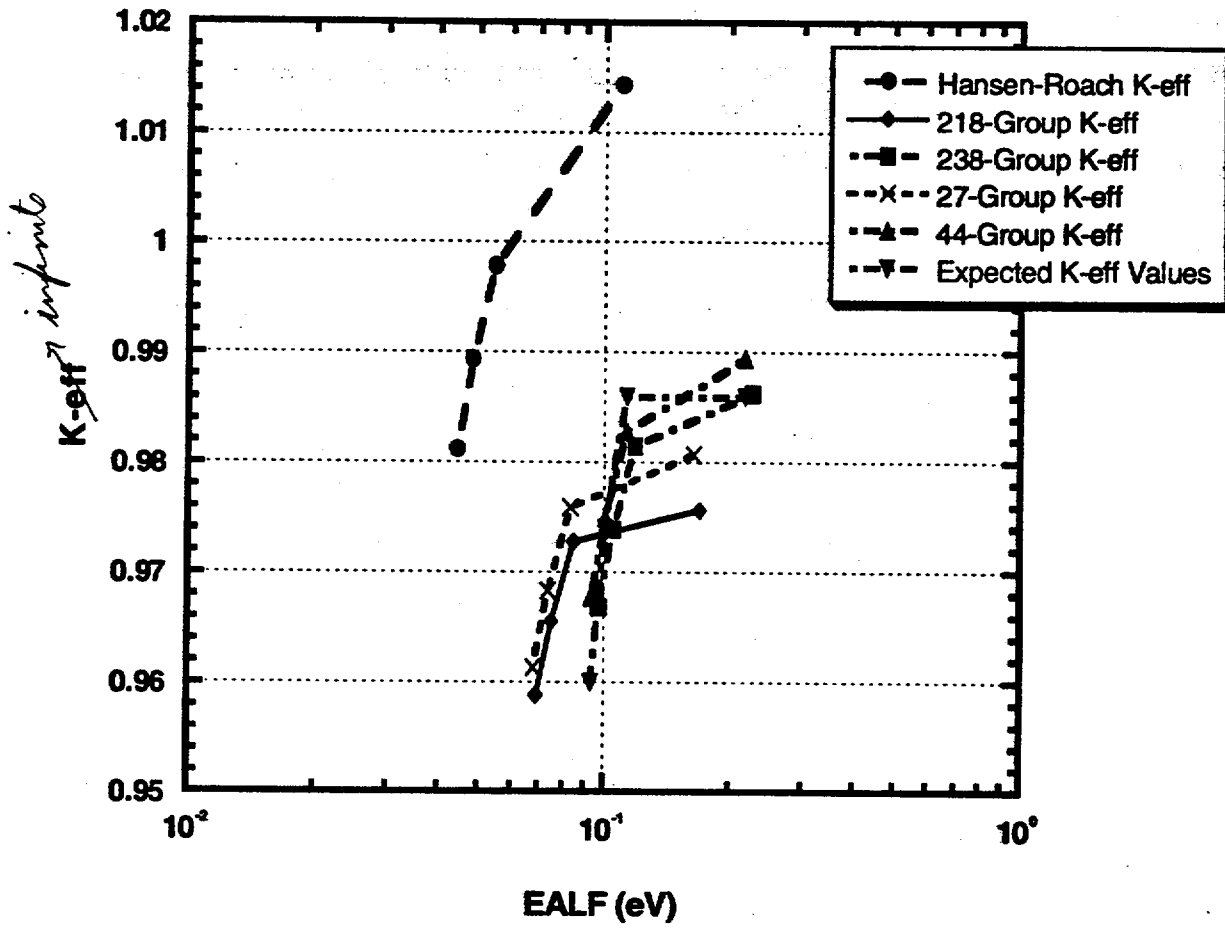


Fig. B.3. PCTR 1.006 wt% k -infinite experiment results.

PCTR 1.071 wt % k-infinite Experiments

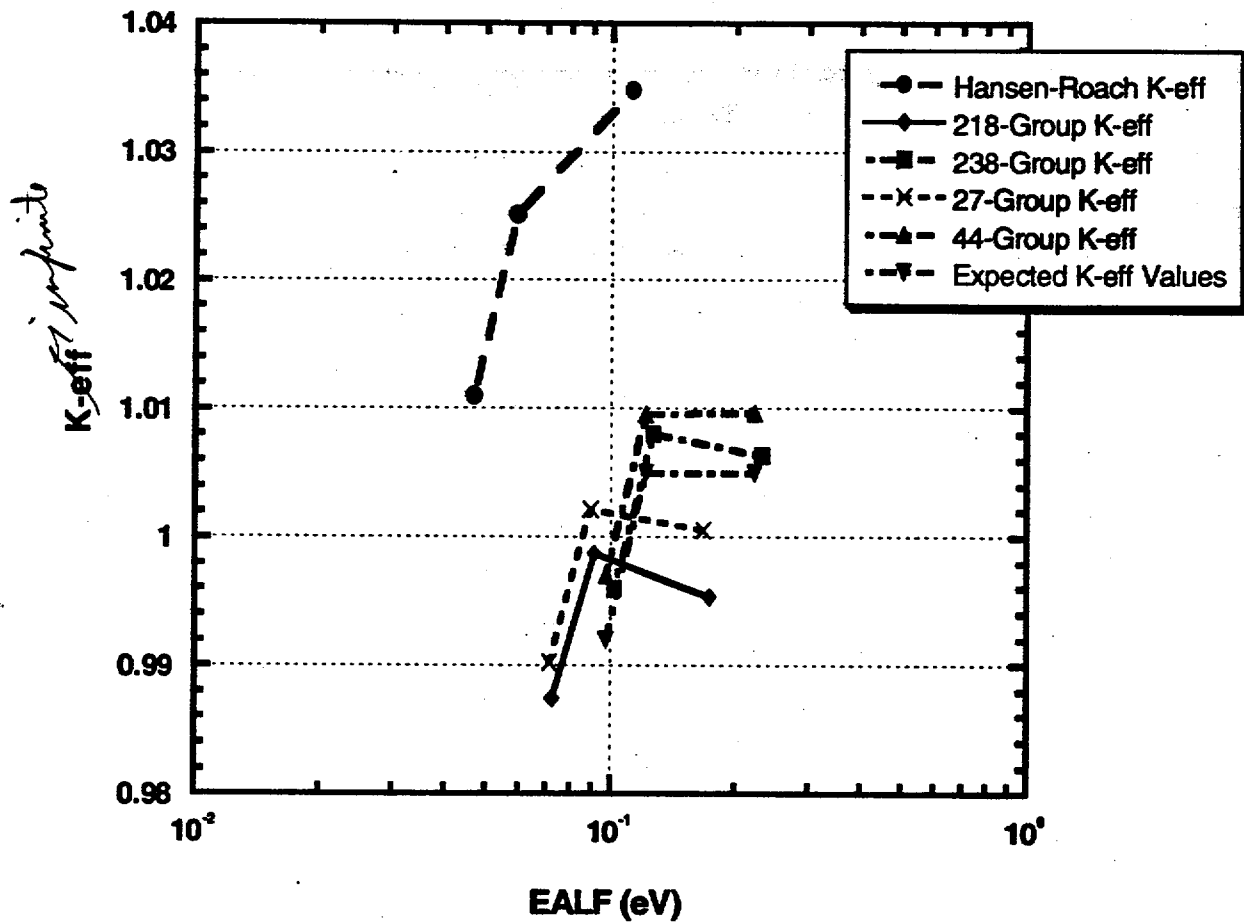


Fig. B.4. PCTR 1.071 wt% k_{∞} experiment results.

PCTR 1.157 wt % k-infinite Experiments

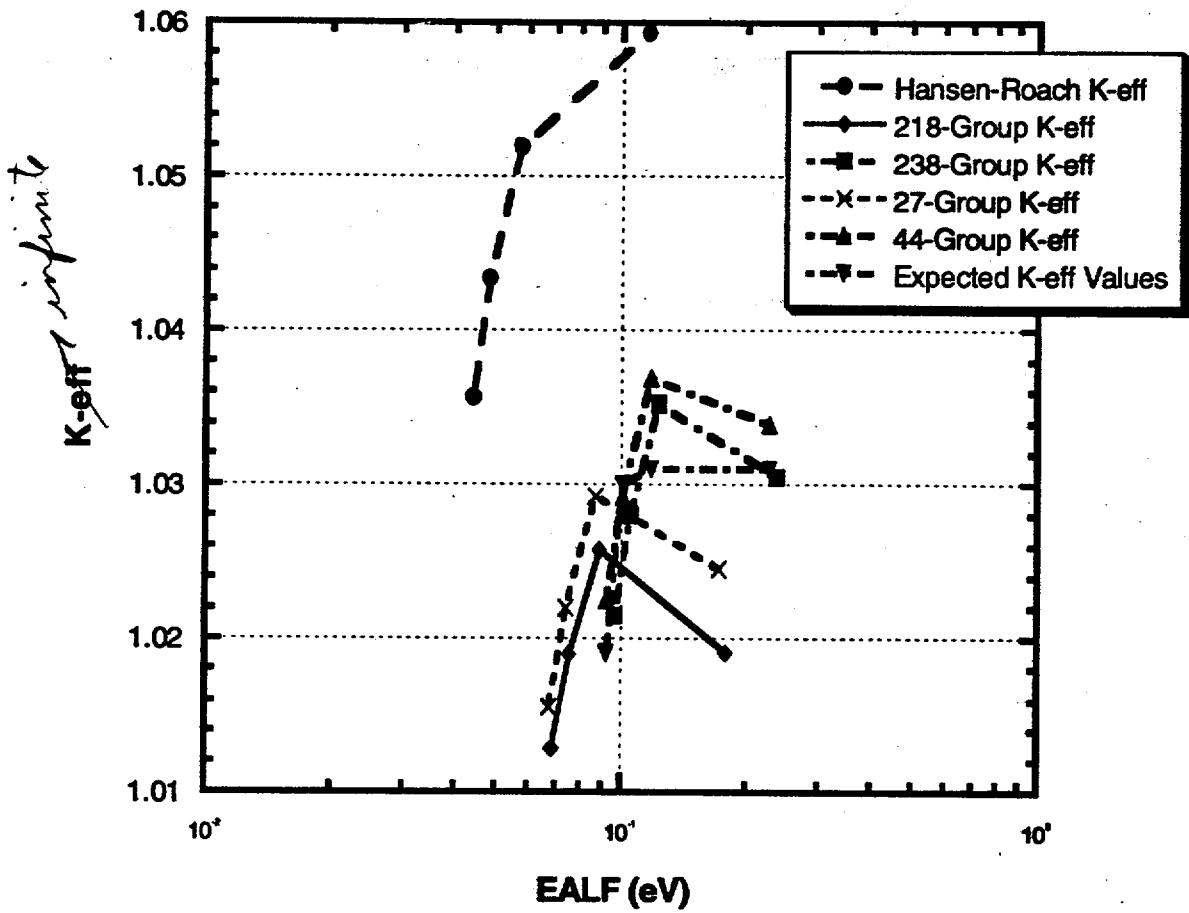


Fig. B.5. PCTR 1.157 wt% *k*-infinite experiment results.

Table E.1 Resonance nuclides in the ENDF/B-V libraries (continued)

Std. comp. alphanumeric name	Nuclide ID No.	Highest order resonance (l value)
CS-133	55133	0
CS-136	55136	0
BA-134	56134	0
BA-135	56135	0
BA-136	56136	0
BA-137	56137	0
LA-139	57139	0
PR-141	59141	0
ND-142	60142	0
ND-143	60143	0
ND-144	60144	0
ND-145	60145	0
ND-146	60146	0
ND-148M	60148	0
ND-150	60150	0
PM-147	61147	0
PM-148M	61601	0
SM-147	62147	0
SM-149	62149	0
SM-150	62150	0
SM-151	62151	0
SM-152	62152	0
SM-154	62154	0
EU	63000	0
EU-151	63151	0
EU-152	63152	0
EU-153	63153	0
EU-154 ^a	63154	0
EU-155 ^a	63155	0
GD-152	64152	0
GD-154	64154	0
GD-155	64155	0
GD-156	64156	0
GD-157	64157	0
GD-158	64158	0
GD-160	64160	0
TB-159	65159	0
DY-160	66160	0
DY-161	66161	0
DY-162	66162	0
DY-163	66163	0
DY-164	66164	0
HO-165	67165	0
ER-166	68166	0
ER-167	68167	0
LU-175	71175	0
LU-176	71176	0
HF	72000	0
HF-174	72174	0

← Add this →